

UNIVERSITÀ DEGLI STUDI DI PADOVA

Dipartimento di Ingegneria Industriale DII

Corso di Laurea Magistrale in Ingegneria dei Materiali

**Optimization of  $K_2ZrF_6$  pretreatment on  
continuous carbon fibers for Al/Mg matrix composites**

OLTJON KARRIQI

Final Year Project

Supervisors:

Prof. IRENE CALLIARI

Prof. ANNE MERTENS

Academic year 2017/2018







## Abstract

Metal matrix composites consisting of an Al/Mg matrix reinforced with carbon fibers offer a remarkable combination of good mechanical properties and low density. However several production issues can be impaired to the poor wettability of carbon fibers by molten metal. In this work, different surface treatments on the carbon fibers are performed in order to derive the best process parameters of both desizing and  $K_2ZrF_6$  treatments. The desizing treatment is meant to remove the polymeric coating on the carbon filaments that could burn in contact with the molten metal giving rise to poor interface cohesion. The  $K_2ZrF_6$  aqueous solution treatment is thought to improve the wettability of the carbon filaments by molten aluminum following a complex sequence of chemical reactions at the fiber-metal interface. The main aim of this work consisted in the optimization of the parameters adopted in the treatment that affect the distribution of the  $K_2ZrF_6$  crystals on the carbon filaments thus affecting the characteristics of the interface due to the rate of chemical reactions locally occurring. In this work is shown that a 5 minutes treatment with a supersaturated solution at  $95^\circ\text{C}$  gave the best results in terms of spontaneous infiltration of molten Al inside the carbon yarns. However an excessive amount of the salt was detected after SEM analysis at the fiber-metal interface. DSC tests were conducted in order to study the sequence of chemical reactions taking place during the interface formation and the obtained results were correlated to the optical microscope and SEM observations.



# TABLE OF CONTENTS

<b>1 INTRODUCTION .....</b>	<b>1</b>
<b>2 STATE OF ART .....</b>	<b>3</b>
2.1 METAL MATRIX COMPOSITES MMCS .....	3
2.1.1 Aluminum/Magnesium matrix reinforced with continuous C fibers.....	4
2.1.2 Interface of a metal matrix composite .....	6
2.2 CLASSES OF CARBON FIBERS .....	7
2.3 SURFACE TREATMENTS AND DESIZING OF CARBON FIBERS .....	8
2.3.1 Oxidative or non-oxidative surface treatment and plasma process .....	9
2.3.2 Sizing carbon fibers .....	10
2.3.3 Desizing of carbon fibers for MMCs .....	12
2.4 THE $K_2ZrF_6$ WETTING IMPROVEMENT .....	14
2.4.1 Issues of Al/C composites.....	14
2.4.2 Effects of $K_2ZrF_6$ treatment .....	16
2.4.3 $K_2ZrF_6$ treatment in literature .....	18
<b>3 EXPERIMENTAL METHODS .....</b>	<b>20</b>
3.1 UTILIZED MATERIALS .....	20
3.1.1 Continuous carbon fibers .....	20
3.1.2 Differential thermal analysis on aluminum .....	20
3.1.3 $K_2ZrF_6$ salt .....	23
3.2 CARBON FIBERS PREPARATION.....	24
3.2.1 C fibers surface observation .....	24
3.2.2 Desizing through heating.....	24
3.2.3 The $K_2ZrF_6$ treatment.....	25
3.3 THERMAL ANALYSIS .....	28
3.3.1 Differential scanning calorimetry (DSC) analysis.....	28
3.3.2 General rules for interpreting DSC thermographs.....	30
3.4 MICROSTRUCTURAL CHARACTERIZATION .....	30
3.4.1 Optical microscope and Stream Analysis Software.....	30
3.4.2 Scanning Electron Microscope .....	32
<b>4 RESULTS.....</b>	<b>33</b>
4.1 CARBON FIBERS DESIZING.....	33
4.1.1 SEM images of sized C fibers.....	33
4.1.2 SEM analysis after desizing.....	35
4.2 $K_2ZrF_6$ TREATMENT RESULTS .....	38
4.2.1 Optical microscope images of treated fibers.....	39
4.2.2 Treated fibers surface SEM analysis results .....	40

4.3 THERMAL ANALYSIS RESULTS .....	47
4.3.1 DSC spectra .....	48
4.4 COMPOSITE SAMPLE MICROSTRUCTURE.....	57
4.4.1 Composite sample optical microscope images .....	57
4.4.2 Composite SEM analysis results.....	58
<b>5 DISCUSSION.....</b>	<b>69</b>
5.1 CARBON FIBERS SURFACE .....	69
5.1.1 Desizing considerations .....	69
5.1.2 Characteristics of $K_2ZrF_6$ treatment.....	70
5.2 INTERFACE FORMATION .....	73
5.2.1 Interpretation of DSC curves .....	74
5.2.2 Microstructure of composite sample.....	76
<b>6 CONCLUSIONS AND FUTURE PROSPECTS .....</b>	<b>79</b>
<b>7 REFERENCES .....</b>	<b>80</b>



# 1. INTRODUCTION

This thesis presents the study of the surface pre-treatments on continuous carbon fibers with the aim of favoring the spontaneous wetting of carbon substrates by liquid aluminum by making use of an aqueous solution of  $K_2ZrF_6$ . Particularly, the work is focused on the optimization of the  $K_2ZrF_6$  process parameters with the purpose of improving the interface cohesion between the carbon fibers and the aluminum. Indeed, the ultimate mechanical properties of all kinds of composites are strongly affected by the characteristics of the interface.

This work is part of a vaster research project by the University of Liège: Métallurgie et Science des Matériaux (MMS) and it partially represents the continuation of a previous work with a published paper by Anne Mertens et al [1].

In the following chapters, the topics here shortly presented will be described. Firstly, chapter 2 will present the state of art on metal matrix composites (MMCs) focusing on Aluminum/Magnesium matrix reinforced with continuous carbon fibers and surface treatments of carbon fibers. Chapter 3 will present the experimental methods utilized in this work while, in chapter 4, the results of the performed test will be reported. The following chapter 5 is meant to present the discussion of the obtained results. Finally, chapter 6 will show the conclusions and the prospects while chapter 7 contains the references.



## 2. STATE OF ART

This chapter is meant to present the state of art of the topics needed for the discussion of the results. The main topics described consist about: metal matrix composites, focusing on Al/C composites; surface treatment and desizing of carbon fibers.

### 2.1 METAL MATRIX COMPOSITES

The growing spread of composite materials stems from the fact that most monolithic materials excel in only a few areas, such as hardness, refractoriness, cost, toughness, ease of processing, etc. Composite materials are developed in order to obtain combinations of mechanical, thermal, or electrical properties that would otherwise not be feasible. Metal matrix composites (MMCs) usually consist of a low-density metal, such as aluminum or magnesium, reinforced with particulate or fibers of a ceramic material, such as silicon carbide or graphite. Compared with unreinforced metals, MMCs offer higher specific strength and stiffness, higher operating temperature, and greater wear resistance, as well as the opportunity to tailor these properties for a particular application. MMCs are increasingly sought for a wide range of applications in the aerospace, automotive, and structural fields because of their several attributes. In comparison to monolithic metallic materials, MMCs offer the following advantages:

- higher strength to weight ratio, which results in significant weight savings;
- higher specific modulus;
- enhanced elevated temperature stability in terms of better creep resistance;
- improved dimensional stability;
- comparable or improved fatigue characteristics;
- enhanced damping characteristics;
- enhanced abrasion and wear resistance.

As presented in Figure 2-1, the types of MMCs can be grouped according to the form of the reinforcements: particulates, short fibers or whiskers, continuous fibers, laminates or sheets, interconnected reinforcement, singular metal core reinforcement.

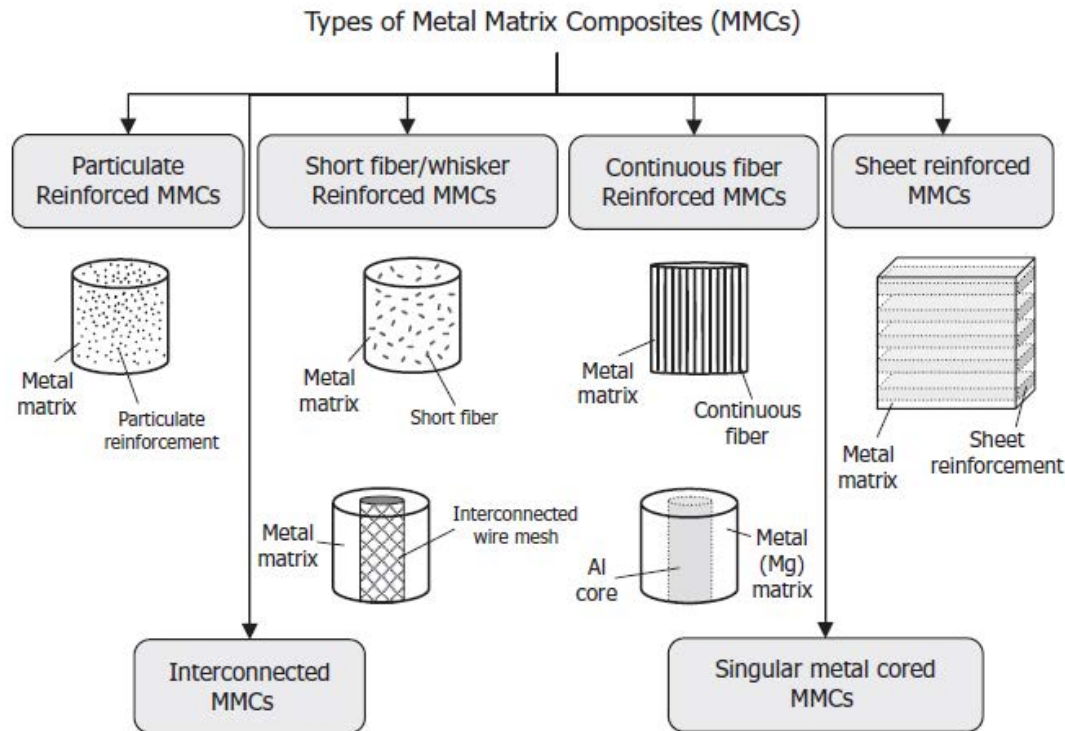


*Fig.2-1: Different types of metal matrix composites [2].*

### 2.1.1 Aluminum/Magnesium matrix reinforced with continuous C fibers

The application of continuous carbon fiber-reinforced aluminum matrix composites (CF/Al) in aerospace, automobile, and electric power cable industries is of considerable interest because of their high specific strength, specific modulus, and low coefficient of thermal expansion. Carbon/aluminum MMC development was initially encouraged by the commercial appearance of strong and stiff carbon fibers in the 1960s. However, carbon and aluminum in combination are difficult materials to process into a composite. A deleterious reaction between carbon and aluminum, poor wetting of carbon by molten aluminum, and oxidation of the carbon are significant technical barriers to the production of these composites [3]. A range of different processes are currently used for making commercial C/Al MMCs: liquid metal infiltration of fiber yarns [4], vacuum vapor deposition of the matrix on spread yarns [5], and hot press bonding of spread yarns sandwiched between sheets of aluminum [3] etc. With both precursor wires and metal-coated fibers, secondary processing such as diffusion bonding or pultrusion is needed to make structural elements.

Squeeze casting also is practicable for the fabrication of this composite [6] when carbon fibers surface pretreatment allow good wettability by the molten metal. Precision aerospace structures with strict tolerances on dimensional stability need stiff, lightweight materials that exhibit low thermal distortion. Carbon/aluminum MMCs have the potential to meet these requirements. In theory, C/Al angle-ply laminates can be designed to provide a coefficient of thermal expansion (CTE) of closely zero by selecting the appropriate ply-stacking arrangement and fiber content. In practice, a near-zero CTE has been realized, but expansion behavior is complicated by hysteresis attributed to plastic deformation taking place in the matrix during thermal excursions [7]. The advent of pitch-based graphite fibers with three times the thermal conductivity of copper suggests that a high-conductivity low-CTE version of C/Al can be developed for electronic heat sinks but also space thermal radiators [8].

Magnesium composites are being developed to exploit essentially the same properties as those provided by aluminum MMCs: high stiffness, light weight, and low CTE. In practice, the choice between aluminum and magnesium as a matrix is usually made on the basis of weight versus corrosion resistance. Magnesium is approximately two-thirds as dense as aluminum, but it is more active in a corrosive environment. Magnesium has a lower thermal conductivity (but still quite high), which is sometimes a factor in its selection. Different types of magnesium MMCs are currently under development such as: continuous fiber C/Mg for space structures, short staple fiber for automotive engine components and low-expansion electronic packaging materials. The production of the continuous-fiber C/Mg composite involves the titanium-boron coating method of making composite wires, physical vapor deposition of the matrix on fibers, or diffusion bonding of fiber-thin sheet sandwiches to make panels [9]. A casting technology exists for C/Mg that involves the deposition of an air-stable silicon dioxide coating on the fibers from an organometallic precursor solution [10]. Magnesium wets the coating, permitting incorporation of the matrix by near-net-shape casting procedures.

In the case of magnesium matrix composites with C fibers reinforcements, wetting is more particularly an issue as the wettability of C substrates by Mg alloys is known to be poor [11,12]. From all of the processes aiming at enhancing the wettability of C fibers, the

deposition of a metallic layer on the fibers appears particularly promising since the wetting of a metal on a metallic substrate is known to be usually adequate [13].

In order to permit the spontaneous wetting of carbon yarns by liquid aluminum, an alternative processing method has been studied in this work, by exploiting the already known effect of a pre-treatment with an aqueous solution of  $K_2ZrF_6$  [14–18]. The  $K_2ZrF_6$  crystals deposited on the C substrate has been shown to dissolve the superficial alumina layer covering the Al bath following a complex sequence of interface reactions that will be illustrated later on. This is recognized to be the main cause of the wetting improvement brought by the  $K_2ZrF_6$  salt. Furthermore other factors such as the cleaning of the surface of the substrate by the fluorides species and the local increase in temperature due to the heat produced by the chemical reactions are thought to have an worth mentioning effect [14]. Nonetheless, the sequence of reactions is modified and the  $K_2ZrF_6$  is consumed to form  $MgF_2$  in occurrence of substantial Mg amount [14]. Consequently, it can be stated that a pre-treatment of the carbon tows with  $K_2ZrF_6$  does not lead to any significant enhancement of the wetting by Al-based alloys containing magnesium [14] or by Mg-based alloys. Considering this impediment in spontaneous infiltration of the carbon fibers reinforcements by liquid Mg, the “Compomag Project” of the MMS department aimed at evaluating the feasibility of using preforms made of carbon yarns pre-infiltrated with pure Al (after pretreatment with  $K_2ZrF_6$ ). Particularly, the aim of the work presented here relay on the optimization of the  $K_2ZrF_6$  pretreatment by tuning the process parameters and studying their effect by making use of DSC (*Differential Scanning Calorimetry*) measurements, optical microscope observations as well as SEM (*Scanning Electron Microscope*).

### **2.1.2 Interface of a metal matrix composite**

Advanced composite materials have the unique combination of outstanding mechanical properties of matrices and reinforcements. The reinforcement/matrix interface in composite materials forms in manufacturing processes and determines the performances of the composite materials. Some reinforcements may not be compatible with matrices in view of their physical and/or chemical properties, which cause premature failure of the composites. The brittleness of the composite systems under load and during crack propagation processes

can be reduced by activating a number of energy-dissipative mechanisms like crack shielding, crack deflection, multiple crack formation, crack branching, debonding and pull-out of the fibers. These processes are known to be particularly operative in the interface between fiber and matrix. In general, consisting of several layers with a complex microstructure, the interfacial regions are either built up by fiber coating or generated during the processing of the composites by chemical reactions.

The complex behavior of the interfaces will be optimum with respect to debonding and pull-out processes denoting the wanted toughness and strength parameters, if both their microstructure and microchemistry are entirely identified and if advanced mechanical testing methods will reveal corresponding structure/property relations.

In MMCs, the interface plays an important role in the load transfer and stress relaxation. Moreover, the thermal expansion behaviors are also affected by the interface further emphasizing its importance.

In this work, the pretreatment of the continuous carbon fibers with  $K_2ZrF_6$  strongly influences the interface between the fibers and the aluminum as a consequence of various chemical reactions depending also on the quantity and the size of the  $K_2ZrF_6$  crystals that are deposited on the fibers.

## **2.2 CLASSES OF CARBON FIBERS**

Carbon fiber is defined as a fiber containing at least 92 wt % carbon, while the fiber containing at least 99 wt % carbon is usually called a graphite fiber [19]. Carbon fibers generally have excellent tensile properties, low densities, high thermal and chemical stabilities in the absence of oxidizing agents, good thermal and electrical conductivities, and excellent creep resistance. They have been extensively utilized in composites in the form of woven textiles, prepregs, continuous fibers/rovings, and chopped fibers. In the latest years, the carbon fiber industry has been growing steadily to meet the demand from different industries such as aerospace (aircraft and space systems), military, turbine blades, construction (non-structural and structural systems), light weight cylinders and pressure vessels, offshore tethers and drilling risers, medical, automobile, sporting goods, etc.

The current carbon fiber market is dominated by polyacrylonitrile (PAN) carbon fibers, while the rest is pitch carbon fibers and a very small amount of rayon carbon fiber textiles [20]. Different precursors produce carbon fibers with different properties. Although producing carbon fibers from different precursors requires different processing conditions, the essential features are very similar. Generally, carbon fibers are manufactured by a controlled pyrolysis of stabilized precursor fibers. Those precursor fibers are first stabilized at about 200–400 °C in air by an oxidization process. The infusible, stabilized fibers are then subjected to a high temperature treatment at around 1000 °C in an inert atmosphere to remove impurities such as hydrogen, oxygen, nitrogen, and other non-carbon elements. This step is commonly called carbonization. Carbonized fibers can be further graphitized at an even higher temperature up to around 3000 °C to achieve higher carbon content and higher Young's modulus in the fiber direction. The properties of the resultant carbon/graphite fibers are affected by various factors such as crystallinity, crystalline distribution, molecular orientation, carbon content, and the amount of defects.

In terms of final mechanical properties, carbon fibers can be roughly classified into ultra high modulus (>500 GPa), high modulus (>300 GPa), intermediate modulus (>200 GPa), low modulus (100 GPa), and high strength (>4 GPa) carbon fibers [20]. Carbon fibers can also be classified, based on final heat treatment temperatures, into type I (2000 °C heat treatment), type II (1500 °C heat treatment), and type III (1000 °C heat treatment). Type II PAN carbon fibers are usually high strength carbon fibers, while most of the high modulus carbon fibers belong to type I.

### **2.3 SURFACE TREATMENTS AND DESIZING OF CARBON FIBERS**

Carbon fibers (CFs) have received much attention lately for their many potential applications in different matrix materials owing to their properties, processability, and recyclability. However, raw CFs need to be treated and/or sized as part of the manufacturing process. Designing a suitable surface-treatment method is a requisite to ensure that the high strength of the CFs is maintained during handling and composite manufacturing. The surface treatment or sizing method is also equally important to guarantee an optimal formation of CF-matrix interface. In fact, when a load is applied to



the carbon fiber composite, the stress is transferred from one carbon filament to another via the matrix material. If a weak fiber resin bond is present, then it will result in poor mechanical properties, such as low interlaminar shear strength, which is attributed to a lack of bonding between the matrix and fiber filaments. Normally, this problem can be overcome by some form of surface treatment of the fiber, but if the bond is too strong, then the composite may become brittle and weak. However, too little treatment and the composite will remain weak, so it is most important to establish an optimum level of surface treatment for a specified fiber and matrix system.

Treatments can be applied by a batch or continuous process and obviously, fiber production will favor the latter. Many methods of oxidative surface treatment have been used including gaseous, solution, electrochemical, plasma and catalytic.

Various forms of non-oxidative surface treatments can be used, including the deposition of an active form of carbon, the deposition of pyrolytic carbon and by grafting a polymer onto the fiber surface.

Factors which must be taken into consideration when choosing a system include the length of time that the surface treatment will take, how practical it is to operate, the cost of the treatment, whether the weight loss is significant and, if the process involves a wet system, then the incorporation of a drying stage.

### **2.3.1 Oxidative or non-oxidative surface treatment and plasma process**

Initially, carbon fiber was only available in a staple form and batch surface treatment processes had to be used, but with the advent of continuous carbon fiber, these were replaced by continuous processes.

Basically, the effect of the oxidation on CFs reveals as the displacement of carbon atoms from their graphitic structures. Air, oxygen diluted with an inert gas, nitrous oxide, nitrous dioxide, ozone, steam or carbon dioxide may be utilized as the gas phase oxidation, but also different liquid phase oxidation techniques or anodic oxidation are implemented in the modern C fibers processing [19]. Actually, when carbon fibers were introduced in a continuous form, anodic oxidation became the favored route for surface treatment, using the conductive property of carbon fiber to act as an anode in a suitable electrolyte bath. An

electric potential is applied to the fiber, sufficient to liberate O<sub>2</sub> on the surface by making use of acid, mildly alkaline or strong alkaline solutions [19].

Whiskerization instead, involves the growth of minute single crystals, such as SiC, Si<sub>3</sub>N<sub>4</sub> and TiO<sub>2</sub> at right angles to the fiber surface in order to promote bonding between the fiber and resin in a composite is the most common non-oxidative surface treatment [19].

Plasma, also called the fourth state of matter, is a partially or fully ionized gas containing electrons, ions and neutral atoms or molecules, where the atoms have so much kinetic energy that the valence electrons are freed by atomic-level collisions [21]. Plasma surface treatment is a dry reaction process and depending on the process conditions, can have the following effects, which may occur concurrently on a carbon fiber surface:

- cleans the outside, creating a hydrophilic surface for enhanced bonding;
- removes the surface layer by a micro-etching process;
- penetrates the top few molecular layers (100 about 10 nm) and modifies the surface, creating a new surface chemistry, enabling improved interfacial adhesion in composites.

Typical gases used to create a plasma include air, O<sub>2</sub>, NH<sub>3</sub>, N<sub>2</sub> and Ar [21].

### **2.3.2 Sizing carbon fiber**

The commercially available CFs are normally coated by a sizing layer on the surface, which usually is either a solution or emulsion consisting of polymeric components. The presence of sizing in the CFs/sizing and sizing/matrix interfaces plays an important role in controlling certain properties of the composites. Conventional sizing such as film formers, emulsifiers, antistatic, and coupling agents is generally designed to protect the fiber surface and promote the adhesion between the fiber and matrix. The sizing could alter the handling of the CFs, which includes protection, alignment, and wettability of fibers. The typical sizing materials include epoxy, polyester, nylon, urethane, and others polymers used to improve inter-filamentary adhesion, aid in wetting out the fiber in resin matrices and act as a lubricant to prevent fiber damage during subsequent textile processing such as weaving [19].

The application of a coating is normally termed either size or finish and can be achieved by:

- deposition from solution of a polymer;
- deposition of a polymer onto the fiber surface by electrodeposition;
- deposition of a polymer onto the fiber surface by electropolymerization;
- plasma polymerization.

The most common form of sizing is the deposition from solution of a polymer onto the fiber surface. The choice of size depends on the resin matrix and some thermoplastics like PEEK will require the ability to withstand high processing temperatures, so epoxy resins are generally used for epoxy matrices while a polyimide would be required for PEEK. To obtain the right handle, applied sizes should not be tacky or brittle and can be achieved by selecting a resin with a suitable epoxy molar mass to avoid the tacky state, or the epoxy could be partly cured [19].

As regards electrodeposition, a preformed polymer with an ionized group is said to be electrodeposited when, under an applied voltage, the polymer is attracted to the oppositely charged carbon fiber an electrolytic cell. A uniform non-conducting layer of polymer with a specified thickness can be applied to the carbon fiber at a controlled deposition rate.

Electropolymerization instead, enables the polymerization of monomers in an electrolytic cell, where the carbon fiber can be made the anode or the cathode. The solvent used to dissolve the monomer must act as an electrolyte and be sufficiently conducting to permit a uniform non-conducting layer of polymer to be applied onto the carbon fiber at a controlled deposition rate and specified thickness [19].

The appearance of sized fibers observed using Scanning Electron Microscope (SEM) is shown in Fig. 2-2. It is easy to notice the presence of an irregular polymeric coating on the surface of any of the filaments composing the yarn.

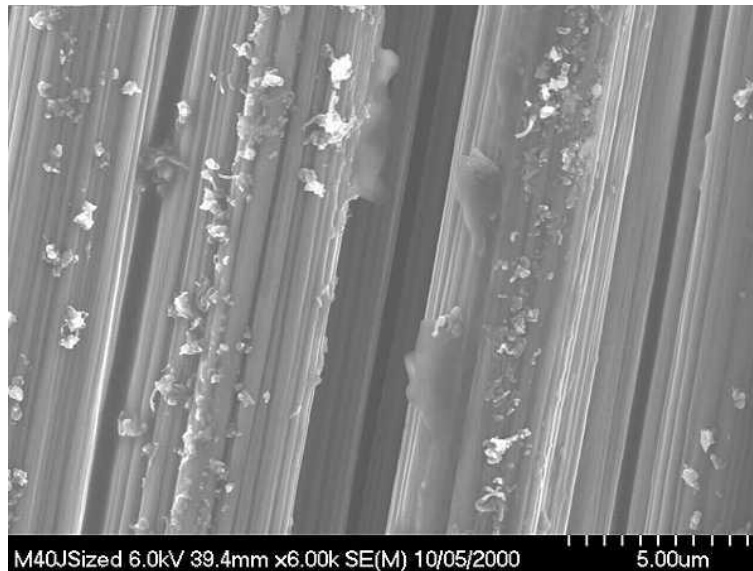


*Fig.2-2: appearance of the sized Toray M40J carbon fibers observed on SEM [22].*

### **2.3.3 Desizing of carbon fibers for MMCs**

The polymeric sizing on the carbon fibers (CFs) could be an issue when it comes to use them as continuous reinforcement for metal matrix. Beside representing an impurity, it could burn when coming into contact with the molten metal and the resulting combustion gases might lead in turn to the occurrence of the porosity in the final composite [23]. For this reason, it is necessary to use CFs specifically dedicated to the processing of MMCs (without sizing) or adopt a desizing process prior to any other treatment.

In the literature there are suggested different desizing processes depending on the commercial polymeric coating characteristics and the degree of surface that is desirable to obtain.

Zhishuang Dai et al. [24] propose an extended desizing process of the commercial Toray T300B and T700SC carbon fibers carried out by acetone extraction at 75 °C for 6 h, with returning rate of 30 min, followed by drying at 60 °C in vacuum oven for 8 h. This process results to be quite complicated and should be recommended for high level of surface purity, for instance when there is the need to perform wetting measurement (contact angle measure).

A similar but shorter desizing treatment using acetone has been conducted by Patankar et al. [25] on Torayca T300-3000 carbon fibers. In order to ascertain the removal of the sizing material, they suggest using Fourier transform infra-red spectroscopy in attenuated total reflectance (ATR) mode. The degree of purity obtainable by this process is quite high, even though, the acetone could not be very efficient in removing some particular resin coatings or could add impurities in the yarn.

A detailed chemical desizing approach is reported by Allred and Wesson [22] conducted on Toray M40J and M60J carbon fibers. In their experiment, the fiber sizings were extracted from 1 to 30 minutes in hot chloroform, acetone, and water. They report that boiling water did not remove the sizing to any measurable extent. Five minutes in boiling chloroform or acetone dropped the surface oxygen content to a constant level of approximately 10%. They also state that one, three, and five minutes in boiling chloroform gave the same results.

A totally different desizing approach is described by Katzman [26] in which the carbon fibers are treated in a furnace at 475°C under argon.

The desizing through heating is claimed to be efficient also by Wang et al. [27] as they use TG test and XRD to estimate the weight loss of Toray T300 carbon fibers due to the removal of organic coating at 450°C for 1 hour under air.

In this work it has been adopted the desizing through heating in furnace under air due to its practicality and good efficiency in short time treatment. The parameters of the process will be described in the experimental methods chapter.

The appearance of desized fibers observed using Scanning Electron Microscope (SEM) is shown in Fig. 2-3. It is worth noting how the surface appears to be clean and smooth if compared to the previous image of sized fibers (Fig. 2-2).

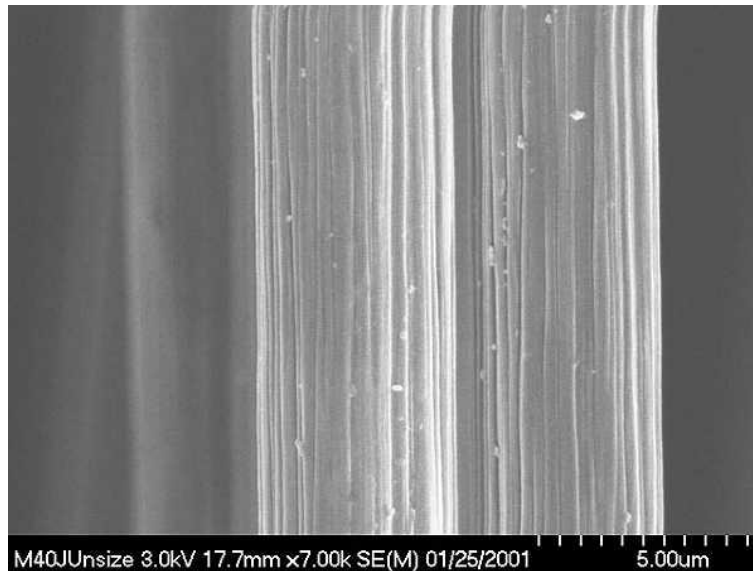


*Fig.2-3: appearance of the desized Toray M40J carbon fibers observed on SEM [22].*

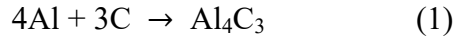
## **2.4 THE $K_2ZrF_6$ WETTING PROCESS**

### **2.4.1 Issues of Al/C composites**

The feasibility of aluminum matrix composite materials has been studied for many years particularly with the aim of providing low-cost processing techniques and high-quality materials. However, as already mentioned, several difficulties have still to be overcome in order to manufacture aluminum matrix composite complex parts, on a large industrial scale (e.g. engine parts for the automotive industry or aerospace industry), by techniques that could be derived from those already used in a light-alloy foundry. Among these difficulties, the key problems seem to be related to the facts that [28]:

- the required fiber-matrix coupling (on a sub micrometer scale) and the part molding must take place simultaneously, in a single short operation, whatever the part complexity, the fiber arrangement and the fiber-volume fraction;
- aluminum poorly wets carbon fibers (as a result, the impregnation of complex-shape fibrous preforms may be impossible or at least incomplete with, in such a case, a significant amount of porosity);

- interfacial chemical reactions often occur at the fiber-metal interfaces even at low temperatures causing fiber degradation and matrix embrittlement (e.g. above  $\sim 500^{\circ}\text{C}$  with formation of  $\text{Al}_4\text{C}_3$  for carbon fibers) following this reaction:



However, the latter is thought to be the reaction responsible of the interface strength between carbon fiber and aluminum matrix. The carbide phase grows as acicular inclusions which embed themselves both in the fibers and in the matrix, thereby forming local bond sites. Carbides nucleate individually on the surface of fiber and increase in size with time and rise in temperature. Non-uniform nucleation results in the formation of colonies of carbides [29]. Large numbers of these carbide crystals or the cohesion bridges strengthen the fiber-matrix bond. Nevertheless, too strong fiber-matrix bond does not allow the energy absorbing mechanisms like fiber pull-out to operate in the interface region causing a decrease in the mechanical proprieties of the final composite that could bring about a brittle behavior. Moreover, because of the incompatibility between carbon fiber and aluminum matrix by the virtue of difference in their thermal expansion coefficients, the C/Al interface is expected to serve as sink for the dislocations [29].

Numerous techniques, usually based on a treatment of the fibers (coating or surface reaction), have been proposed to promote carbon fibers wettability by liquid aluminum and to prevent extensive interfacial reactions. The most efficient are: (i) a metal coating (Ag, Ni, Cu) deposited on the fiber surface by electrolysis of a solution or impregnation with a suspension [30]; (ii) a surface treatment by liquid sodium or Na-K alloys eventually followed by a tin-based alloy coating [31]; (iii) a chemical vapor deposition of titanium-boron compound or of titanium carbide or of a titanium carbide [32]. However, thin metal coatings poorly protect the fibers against the attack by aluminum, and the resulting intermetallic compounds or carbides can still brittle the matrix. Thus, the coating has to be continuous and rather thick (typically about  $1\ \mu\text{m}$ ), with the disadvantage of yielding a significant increase in the material density when the volume fraction of fibers is high [15]. Nevertheless, the industrial scale-up of these techniques seems to be problematic in as

much as most of them must be performed either under inert atmospheres or under pressure, requiring too great an increase in cost.

The technique presented in this work is based on economical and easy pre-treatment of the carbon fibers (as yarns) with an aqueous solution of  $K_2ZrF_6$ . Water is then removed by drying in air, the fluoride precipitating from the solution and remaining spread along each fiber. This treatment does not involve any restrict atmospheres or any long process so it appears to be interesting in terms of large scale production as a continuous process.

#### **2.4.2 Effects of $K_2ZrF_6$ treatment**

The efficiency of the  $K_2ZrF_6$  process, in terms of wetting improvement, has been established by Rocher et al. on the basis of both preform impregnation experiments at laboratory scale and sessile drop experiments [14,28]. When carbon yarns are treated with an aqueous  $K_2ZrF_6$  solution in order to obtain a deposit of a few milligrams of  $K_2ZrF_6$  crystals per  $cm^2$  after evaporation of the solvent, and then put in contact with the surface of a bath of liquid aluminum, the following mechanisms are supposed to occur [14]:

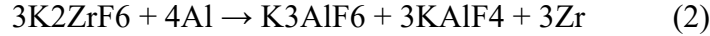
1. the alumina thin layer coating the liquid metal is dissolved by the fluorides which are released by the reaction occurring between  $K_2ZrF_6$  and liquid aluminum;
2. the carbon fiber surface is cleaned and/or activated by these fluorides;
3. the gas phase involved in the wetting phenomenon is advantageously modified by gaseous fluoride species formed from  $K_2ZrF_6$ ;
4. the heat of the exothermic reactions that take place is high enough to increase the temperature locally giving rise to a contact angle decrease.

Although these four mechanisms can be expected to contribute to some extent to the wettability improvement, the first one is thought to be predominant. The contact angle and hence the wettability between carbon substrates and liquid aluminum depends on the thickness of the alumina layer as shown by the fact that [14]: (i) it is lower when aluminum has been treated with sodium hydroxide prior to performing the sessile drop experiment (in such a case the thickness of the alumina layer is thought to be of the order of 2 nm), and (ii) at a given temperature, it is lower as oxygen pressure in the gas phase is low. The aim of



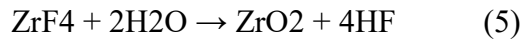
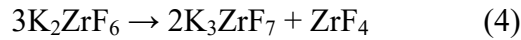
K<sub>2</sub>ZrF<sub>6</sub> is therefore to dissolve the alumina layer allowing a direct contact between the liquid metal and the carbon fibers.

Lundin and Bushe [33,34] have established that the sequence of chemical reactions taking place at high temperatures between pure aluminum and K<sub>2</sub>ZrF<sub>6</sub> can be represented by the following equations:



Moreover, in their experimental results, Rocher et al. [14] observed that when aluminum and K<sub>2</sub>ZrF<sub>6</sub> powders are mixed in the stoichiometric ratio corresponding to Equation (2) and heated at 700 °C (either in air or under vacuum), the X-ray diffraction analysis confirms the occurrence of KAlF<sub>4</sub>, K<sub>3</sub>AlF<sub>6</sub> and Al<sub>3</sub>Zr in the reaction products.

The alumina layer should be thin enough to permit a reaction between liquid aluminum and K<sub>2</sub>ZrF<sub>6</sub>, allowing the reaction products (i.e. particularly K<sub>3</sub>AlF<sub>6</sub>) to dissolve the alumina layer letting a direct contact between the liquid metal and the carbon fibers. Moreover, the kinetics of thermal decomposition of K<sub>2</sub>ZrF<sub>6</sub> can be amplified at high temperatures leading to the formation of several fluoride species according to the following equations:



the latter taking place when the experiment is performed in air. The hydrogen fluoride which is released by reaction (5) could also react with alumina according to the following equation proposed by Rocher [14]:



thus dislocating the oxide layer and allowing wetting of the carbon fiber substrate by liquid aluminum.

### 2.4.3 $K_2ZrF_6$ treatment in literature

Despite the amount of studies conducted on the wettability improvement brought about by the  $K_2ZrF_6$  pre-treatment on the carbon fibers in favoring spontaneous infiltration of molten aluminum inside the C yarns, there is a lack of data regarding the process parameters treatment. Therefore it was decided to focus this work on the optimization of this pre-treatment in order to identify the optimal process parameters that permit to obtain the best possible interfacial cohesion between the C fibers and the Al matrix. Before going onto the experimental methods adopted, in this subsection will be presented the most used process parameters found in literature.

The main parameters of this pre-treatment are: the solution concentration, the temperature, the dip-in time and the level of stirring. The solubility curve of  $K_2ZrF_6$  in water reported in fig.2-2 shows that the solubility of the salt is strongly affected by the value of the solution temperature, especially in the range between 80 °C and 100 °C. The maximum quantity of salt that can be dissolved is approximately 0.25 kg per  $H_2O$  liter at temperature values close to the water boiling point.

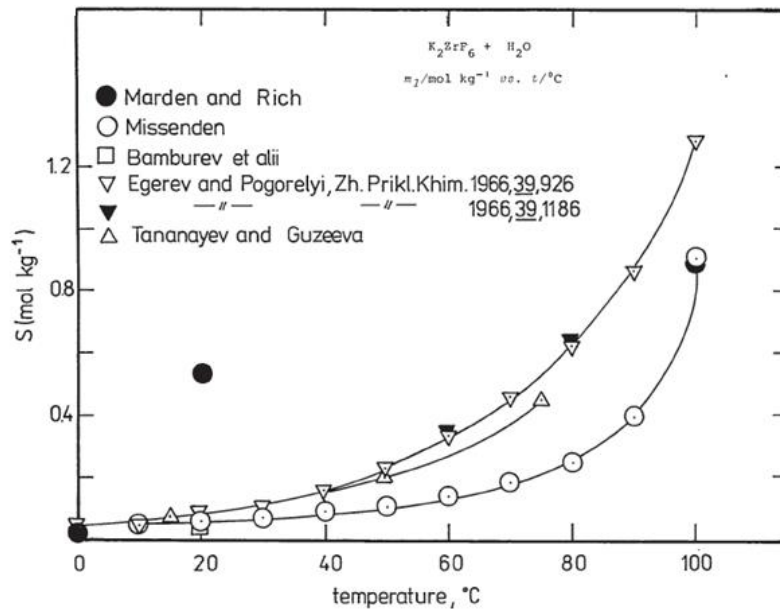


Fig.2-2:  $K_2ZrF_6$  solubility curve in  $H_2O$  [35].

The most common process parameter found in literature refers to a temperature close to 95-100 °C (supersaturated solution) with 2 min dip-in time. Mertens et al. [1] used slightly supersaturated solution at 95 °C and 2 min of dip-in time, Schamm et al. [15] instead did the treatment at value of temperature solution of 80 °C with no indication of the concentration or stirring level. The latter indeed, strongly influence the homogeneity of the solution and hence the  $K_2ZrF_6$  crystal deposition on the C fibers. In this work, different process parameters will be tested and their influence reported in the results chapter.

## **3. EXPERIMENTAL METHODS**

### **3.1 UTILIZED MATERIALS**

In this section will be given all the specific technical information regarding the materials utilized in the experimental work as well as the preliminary analysis performed in order to have a better data quality.

#### **3.1.1 Continuous carbon fibers**

In order to select the type of fiber that gives the better results in terms of surface treatment quality and cohesion strength once combined with molten aluminum, in the first part of the work were used 2 different types of fibers: TORAY 300B, 3000-40B, and TENAX HTA 5131, F12000 800TEX. The technical datasheets of those fibers will be provided in the Annexes chapter (chap 8.) however, important basic information can be individuated in the fibers nomenclature. Indeed, by considering the fibers produced by Toray company, the digit 300B indicates the yarn type, in this case polyacrylonitrile (PAN) fibers, the letter B states that the yarn is untwisted, 3000 refers to the number of filaments, while the last part of the nomenclature designates the sizing type and level, as well as the performed surface treatments. The fibers produced by Tenax company are also PAN based with untwisted yarn however, the main difference with the Toray fibers is in the number of filaments being 12000 in this case as well as the sizing type and surface treatment adopted. As the number of filaments is 4 times greater than the previous ones, this aspect will have a notable impact not only on the desizing process, but also on the  $K_2ZrF_6$  as will be described later on. From the Tenax official website is it indicated that the HTA 5131 fibers are sized for epoxy matrix. Therefore, they can be used in epoxy, phenolic, PBT, polycarbonate, polyethylene, polypropylene, and PPS. However with an efficient desizing process, the majority of carbon fibers can also be used as reinforcements in metal matrix.

#### **3.1.2 Differential thermal analysis on aluminum**

The chemical composition of the aluminum utilized for producing the composite is very important as it strongly influences the type and rate of chemical reactions at the interface

between the metal and the carbon substrates. When using an Al-Si alloy, either aluminum or silicon is expected to react with  $K_2ZrF_6$ . However, it has been established that no reaction occurs between  $K_2ZrF_6$  and silicon [14]. The eventual presence of magnesium is undesirable because it weakens the C fibers and causes the composite to become highly sensitive to corrosion [36]. Therefore, in this work it has been decided to study the behavior of the pure commercial aluminum instead of alloys and the study is focused on pure bulk Al combined with pretreated carbon fibers. Before starting to perform thermal analysis on the composite it is necessary to have the Differential Thermal Analysis (DTA) curve of the aluminum only.

Thus, small Al chips were cut from different zones of the bulk piece of aluminum and inserted into an alumina crucible in the DTA instrument. The main aim of the test relies on obtaining the exact melting temperature but also checking for eventual unexpected reactions or any presence of inhomogeneity in the aluminum piece. The heating was conducted after vacuum was made in the instrument's chamber, under an argon flux. The test was performed with 3 different samples with the parameters reported in Tab. 3-1.

*Tab. 3-1: DTA test parameters of the pure commercial aluminum.*

<i>Sample mass [mg]</i>	<i>Temperature range [ °C]</i>	<i>Heating rate [ °C/min]</i>
172.9	19 - 720	5
131.2	19 – 750	10
150.5	19 – 800	10

The most significant curve is reported in Fig. 3-1. In this case, the initial mass of the sample was 131.2 mg and no noteworthy variations were noticed after the end of the test. The heating was conducted with an increasing rate of 10 °C/min until the final of 750 °C that will be also the parameters adopted in the following DSC tests.

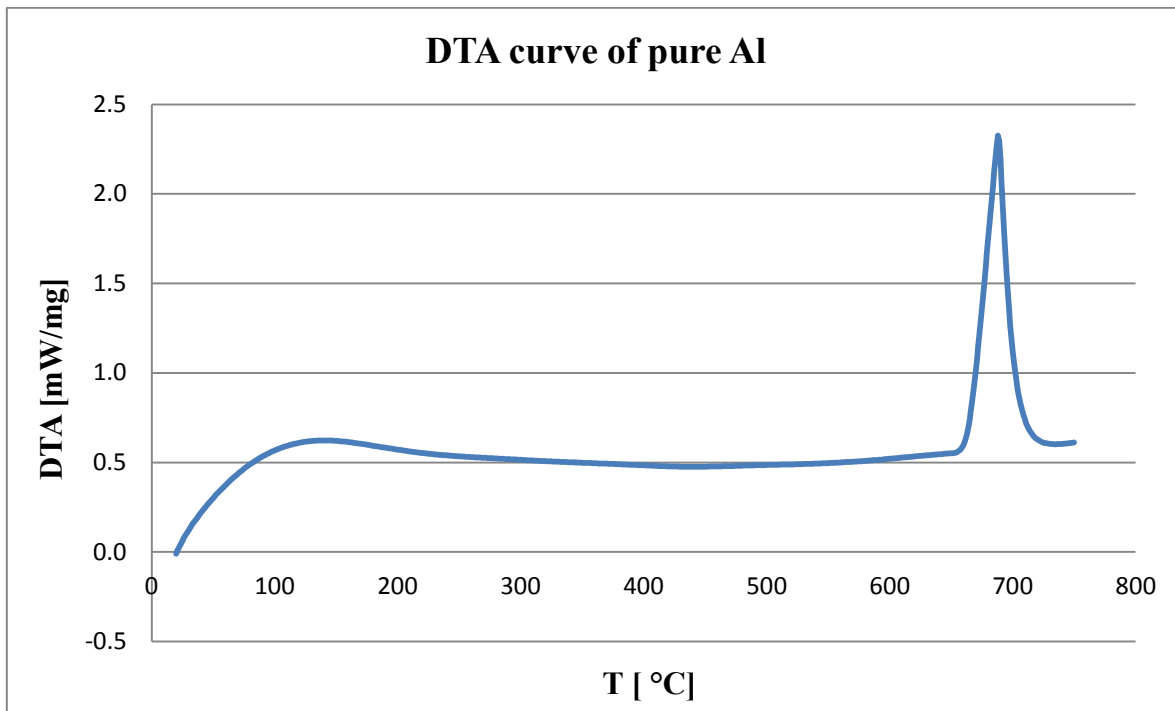


*Fig. 3-1: DTA curve of the pure commercial aluminum sample.*

From the heating DTA curve, it is immediately possible to individuate the melting peak as a consequence of an endothermic reaction. The melting begin at 660.7°C as expected, while the temperature value of the peak is 688.2°C which is supposed to be the ending of melting. The shape of the peak indicates the presence of small impurities in the sample due to the commercial purity level. However their concentration is non-significant to represent an issue in this work. In the first part of the curve there is a slight hunching due to the evaporation of the water presence contained in the sample surface.

The DTA were performed with the NETZSCH STA 449 C® (Fig. 3-2), following standard DIN 51 007. The difference of temperature between is measured by means of thermocouples and expressed into specific heat flux in mW/mg.



*Fig. 3-2: NETZSCH STA 449 C® DTA machine.*

### **3.1.3 $K_2ZrF_6$ salt**

Potassium hexafluorozirconate ( $K_2ZrF_6$ ) is white crystalline powder salt and it is mostly used in metal processing, as a catalyst in chemical manufacture, and for other uses. It is slightly soluble in water at ambient temperature, but its solubility strongly increases close to the water boiling point. The resulting solutions contain moderate concentrations of hydrogen ions and have pH of less than 7.0. Thus,  $K_2ZrF_6$  reacts as acids to neutralize bases. Its neutralizations generate heat, but less or far less than is generated by neutralization of inorganic acids, inorganic oxoacids, and carboxylic acid. Usually  $K_2ZrF_6$  do not react as either oxidizing agents or reducing agents but such behavior is not impossible. The melting point of  $K_2ZrF_6$  is 840 °C and its density is approximately 3.5 g/cm<sup>3</sup>.

## **3.2 CARBON FIBERS PREPARATION**

The most of the experimental work regards the preparation and the treatment of the carbon fibers. Thus, this section is meant to describe the preliminary analysis done on the C fibers as well as the desizing process followed by the  $K_2ZrF_6$  treatment.

### **3.2.1 C fibers surface observation**

As already mentioned, the utilized carbon fibers are characterized by polymeric sizing that must be removed before proceeding with the aqueous solution treatment. Thus, the surface of the as received fibers was observed using the Scanning Electron Microscope (SEM) in order to compare it with the one after the desizing process, i.e. evaluate the effectiveness of the desizing treatment. Indeed, the appearance that the fibers are supposed to have after desizing has already been shown in Fig. 2-3.

Observations were carried out with a Phillips XL30 FEG-ESEM® in secondary electrons mode. The carbon fibers were fixed in an aluminum sample carrier, i.e. a conductive material to avoid the accumulation of electrical charges on the fibers. The carbon filaments composing the yarn have an average diameter of 7  $\mu\text{m}$  and the polymeric coating on their surface is in the order of a few tens of nanometers hence, the observation is quite difficult considering also that the filaments might move due to electrostatic effects. The C filaments cannot be pasted on the sample holder because the glue would affect the surface appearance. The adopted solution was to paste half of the length of the fibers and observe the unstacked filaments.

### **3.2.2 Desizing through heating**

The desizing process is quite critic as it can cause unexpected damage of the carbon filaments or introduce impurities. In literature it is suggested to perform the desizing through heating at a temperature above 450 °C [27], nevertheless, at temperatures close to 600 °C the carbon starts to react with oxygen contained in the air to give carbon dioxide with the consequence of irreversible damage of the filaments surface. The vacuum treatment besides being expensive has to be avoided because the gases that form due to the



evaporation of the polymeric coating must be evacuated using air circulation. Furthermore, the oxygen is needed to react with the coating and remove it with gas formation, otherwise it would react with the C filament surface.

For this reason, a resistance heating furnace with air circulation was used to perform the desizing of the carbon fibers. The furnace has a maximum power of 12 kW and it has temperature value and heating rate control system. In order to avoid any fiber damage it was selected to perform the treatment at 500 °C using the maximum heating rate and maintain this temperature value for different times. The aim in this case was to identify the minimum time required to total remove the polymeric coating. The 2 different carbon fibers were cut into 10 cm length samples and placed in the furnace and heated up with the parameters reported in Tab 3-2.

*Tab. 3-2: Desizing test parameters.*

<i>Final Temperature [ °C]</i>	<i>Isothermal time [min ]</i>	<i>Heating rate [ °C/min]</i>
500	5	15
500	60	15
500	120	15

### **3.2.3 The $K_2ZrF_6$ treatment**

This subsection describes the experimental procedure of the surface pre-treatment of the carbon fibers with the aqueous solution of  $K_2ZrF_6$  that follows after the desizing process.

As already mentioned in the state of art, this pre-treatment is thought to favor the spontaneous wetting of the C fibers by the molten aluminum. Indeed, the  $K_2ZrF_6$  has been shown to dissolve the superficial alumina thin layer covering the liquid Al thanks to a complex sequence of reactions. However, in order to have good interface cohesion, i.e. obtain an optimal infiltration of the molten Al into the C yarn, it is crucial to control the distribution of the  $K_2ZrF_6$  crystals deposited on the C fibers surface by controlling the process parameters of the treatment.

Two different types of fibers as well as diverse process parameters were tested during this experimental process with the aim of studying their influence on the crystal size and their

distribution. The main parameters of the treatment are: the solution concentration, the temperature, the dip-in time and the level of stirring. The solubility curve of  $K_2ZrF_6$  in water reported in Fig.3-3 shows that the solubility of the salt is strongly affected by the value of the solution temperature, especially in the range between 80 °C and 100 °C. The maximum quantity of salt that can be dissolved is approximately 0.25 kg per  $H_2O$  liter at temperature values close to the water boiling point.

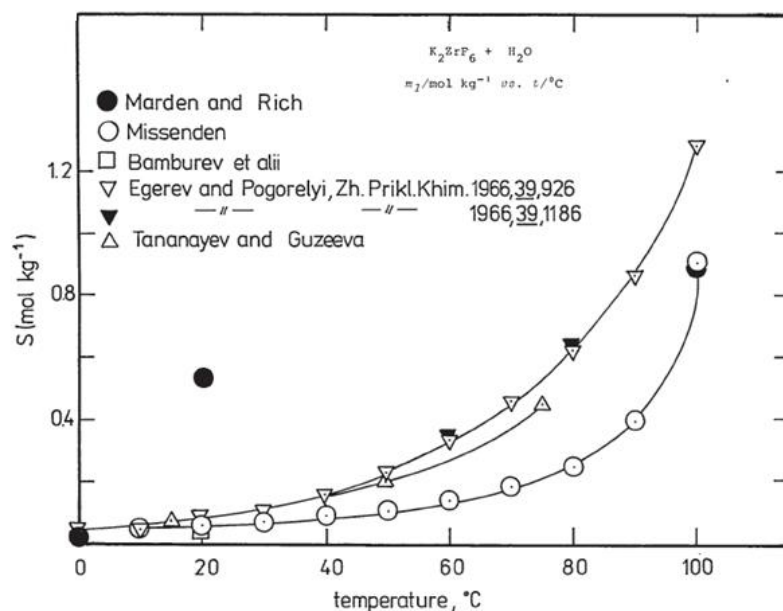


Fig.3-3:  $K_2ZrF_6$  solubility curve in  $H_2O$  [35].

The materials utilized for the treatment are:

- $K_2ZrF_6$  salt in powder;
- desized carbon fibers;
- distilled water;
- 0.5 l beaker;
- heating plate with temperature and magnetic stirring control;
- thermometer.

The first step of the process consists in preparing the solution within the beaker by weighting and mixing the solute and the solvent. As an initial experiment it has been decided to make a slightly supersaturated solution. Therefore, after mixing 50 grams of  $K_2ZrF_6$  in 200 ml of water, the solution contained in the beaker was heated up at 95 °C by

making use of the heating plate with a medium constant level of magnetic stirring. The magnetic stirring and the thermocouple placed inside the solution make it possible to verify that the system reaches a constant regime with a good level of solution homogeneity. Only after reaching a steady value of the solution temperature it is possible to immerse the carbon yarn into it and start measuring the dip-in time.

In the first test, the desized C yarns of 10 cm length were kept for 2 min inside the heated solution before being dried up at 100 °C under air for 1 hour in an oven.

Although the solution preparation is quite easy, some difficulties may come up due to the poor cohesion of the carbon yarn that tend to fall apart during the process, making it impossible to fully control the uniformity of the  $K_2ZrF_6$  crystals distribution on the C fibers surface. Furthermore, when dealing with supersaturated solution, there is always an excess of undissolved salt that tends to deposit not only at the bottom of the beaker, but also on the carbon yarns without properly sticking on the carbon filaments surface. This makes it necessary to manually shake the C yarns after extraction from the solution, to avoid an excessive non-uniform salt deposition.

After this first test, the desized fibers were also tested with different values of the solution temperature and the dip-in time as reported in Tab.3-3. The influence of those parameters will be discussed in chapter 5.

*Tab.3-3:  $K_2ZrF_6$  process parameters.*

<i>Solution concentration</i> [g/100cm <sup>3</sup> ]	<i>Temperature</i> [ °C]	<i>Dip-in time</i> [min]	<i>Level of stirring</i> [-]
25	95	2	Low
25	80	2	Low
25	95	1	Medium
25	95	5	Medium

At the end of the surface treatment the carbon fibers were fixed in a sample carrier support in order to observe them using SEM. The so prepared sample is shown in Fig. 3-4.



*Fig. 3-4: surface treated C fibers prepared for SEM analysis.*

### **3.3 THERMAL ANALYSIS**

Thermal analysis is a family of techniques used for studying the thermophysical and kinetic properties of materials. They can be used with composite materials to determine properties of the matrix material that are important for the analysis of the composite as a whole, but also to study the reactions occurring during the interface formation.

#### **3.3.1 Differential scanning calorimetry (DSC) analysis**

Differential scanning calorimetry (DSC) is a technique that measures the difference in the heat flow to a sample and to a reference sample as a direct function of time or temperature under heating, cooling or isothermal conditions. It can be used with composites and composite precursors to study thermodynamic processes and kinetic events.

In this work, DSC measurements following standard DIN 51 007 were performed using NETZSCH DSC 404 C® (Fig.3-5). In this machine, the sample and the reference are heated from the same source and the temperature difference is measured. This signal is converted to a power difference using the calibration sensitivity. The difference of temperature between the sample and the reference is measured by means of thermocouples

and first expressed in  $\mu\text{V}$  (thermal voltage) and then converted into heat flux, expressed in mW.

The DSC tests completed in this work have both the aim of studying the sequence of reactions that occur between the system of pure aluminum and C fibers treated with  $\text{K}_2\text{ZrF}_6$  as well as producing small composite samples that will be later observed using optical microscope and SEM. For those analyses was utilized boron nitride crucible (BN) because alumina crucible could react with the salt contained on the fibers causing crucible damage and/or measurements errors.

Small pieces of bulk Al were cut and inserted in the BN crucible along with short portion of C fibers after they were treated with the aqueous solution of  $\text{K}_2\text{ZrF}_6$ . The positioning of the materials in the crucible affects the result of the reactions because the C fibers that will not be in contact with the aluminum will not react causing no interface formation. Thus, carbon fibers and Al piece should be positioned in order to allow the metal to entirely cover the carbon filaments once melted.



*Fig. 3-5: NETZSCH DSC 404 C® machine.*

### **3.3.2 General rules for interpreting DSC thermographs**

The peak of a phase transformation may be endothermic or exothermic, depending in whether the chemical transformation absorbs or release thermal energy. In the thermal curves presented in this work, exothermic heat flow is shown down on the y-axis (vice versa the endothermic peaks are shown up in the y-axis).

For a given peak, only the first slope considered to determine the characteristic temperatures of the beginning and the end of the transformation. The second slope corresponds to a relaxation phenomenon that has no physical significance for the phase transformation.

The point where the peak starts deviating from the baseline indicates the onset of a phase transformation. The transformation end when the considered peak reaches the maximum of its amplitude.

When several peaks are superposed in the same temperature range, a deconvolution allows distinguishing these peaks, even if this operation remains delicate.

## **3.4 MICROSTRUCTURAL CHARACTERIZATION**

### **3.4.1 Optical microscope and Stream Analysis Software**

The first step that follows the DSC measurements is the samples preparation for an optimal interface observation. Every small composite sample obtained at the end of DSC measurements, was first fixed in a metallic spring in order to maintain the correct cross section exposure. After that, it was embedded in phenolic conductive resin in the chamber of the mounting machine (Struers CitoPress 1®) to realize an electron conductive sample necessary for SEM analysis. The adopted process parameters were the ones suggested from the product manual both for heating: 180°C, 8 min, 100 bar; and for the cooling phase: max cooling rate, 2 min duration.

The final product was a cylinder shape sample which must be polished so that the sample cross section could reach the lowest surface roughness possible allowing a good observation especially during SEM analysis. The polishing process is portioned in 5 stages differenced by the abrasive sheets and the different lubricant products and it was

extrapolated from the polishing manual of pure aluminum and its alloys. However, some changes were made in order to avoid any fibers pull-out, so it is reassumed in his main parameters as follows.

- 1) Grind with 240-grit SiC water-cooled paper, 240 rpm, 20N per specimen, 1 min.
- 2) Polish with 9- $\mu\text{m}$  Diamond on an Ultra-Pol (silk) cloth, 150 rpm, 20 N/ specimen, 4 minutes (contra rotation).
- 3) Polish with 3- $\mu\text{m}$  Diamond on a Trident cloth, 150 rpm, 20N / specimen, 3 minutes (contra rotation).
- 4) Polish with 1- $\mu\text{m}$  Diamond on a Trident cloth, 150 rpm, 20N / specimen, 3 minutes (contra rotation).
- 5) Polish with 0.05- $\mu\text{m}$  Colloidal Silica on a Microcloth pad, 120 rpm, 20N / specimen, 4 minutes (contra rotation), water cooling last 30 seconds.

During every single step, the samples were cleaned using ethyl alcohol.

The so produced samples were first observed with an Olympus BX60M® optical microscope. The embedded samples are displayed in Fig. 3-6.

Primary, overviews of the whole surface of the cross-section of the samples were taken with low level of magnification to individuate the areas where the interface between C fibers and Al matrix could be better observed. Secondly, higher magnifications were used to observe the characteristics of the so individuated interface areas and the degree of cohesion between the C filaments and the matrix. The Stream Analysis software was used to analyze the elaborated pictures to distinguish the holes caused by dis-uniform melting from the C filaments and to estimate the interface diameters. Finally, the zone between the filament and the matrix was observed using with polarized light at 100X magnification.



*Fig. 3-6: embedded composite samples.*

### **3.4.2 Scanning Electron Microscope**

Observations were carried out with Phillips XL30 FEG-ESEM® in order to understand the reaction between the carbon filaments and the metallic matrix.

Images were taken in Secondary Electrons mode for direct observation. Profiles compositions were obtained with EDS (Energy Dispersive Spectrometry) to better understand the composition of the various zones of the microstructure.

The samples were the same prepared for the optical microscope observation with the only difference of adding two tracks painted with a silver painting to enhance the evacuation of the electrical charges during the analysis. For these observations, the samples were placed on a special support to ensure that the sample does not move during the entire process.



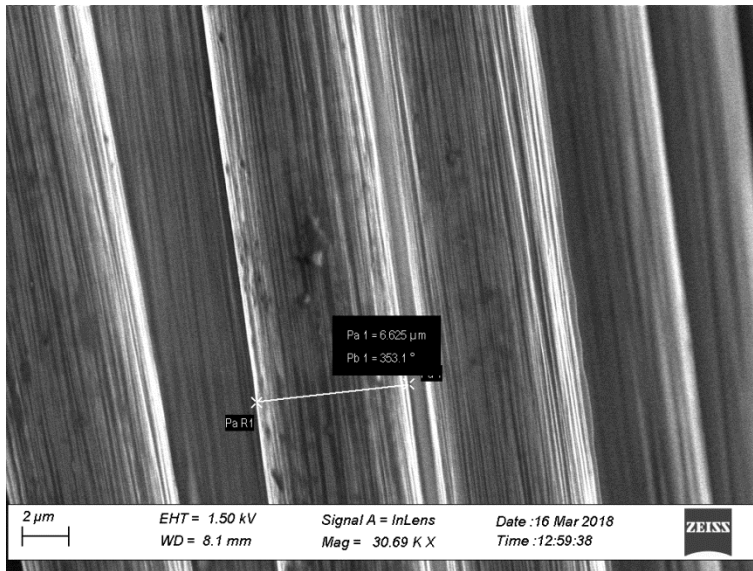
## **4. RESULTS**

### **4.1 CARBON FIBERS DESIZING**

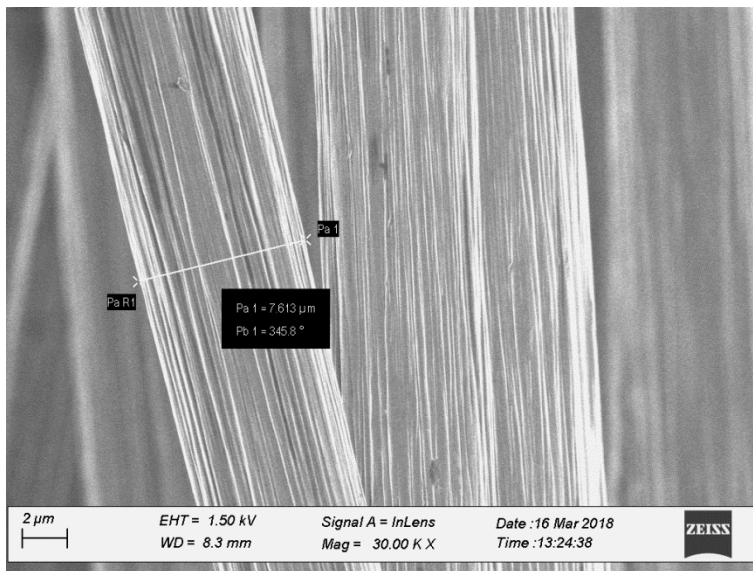
The first section of this chapter presents the analysis made on the carbon fibers prior to the treatment with the aqueous solution of  $K_2ZrF_6$ . SEM analysis have been conducted to detect the characteristics of carbon fibers surface before and after desizing in order to evaluate the efficiency of the adopted process. In this case the usage of the optical microscope is not recommended because the polymeric coating covering the C filaments is in the order of a few tens of nanometers which make it impossible to be observed with the level of magnification performed by optical microscope. Even with the level of magnification provided by SEM, it might be difficult to observe the polymeric coating considering that it is not uniformly distributed on the surface of the C filaments.

#### **4.1.1 SEM images of sized C fibers**

Direct SEM observations have performed on the both as received carbon yarns (without any treatment). The surface of the C filaments is characterized by discontinuous presence of polymeric sizing that appears with irregular shape. The polymeric coating is difficult to detect especially for the TORAY FT300B fibers (Fig. 4-1b), probably because in this case it was adopted to have a very thin coating. It is worth noting that also the manipulation of the yarns can affect the level of purity of the carbon filament surface. Indeed, as shown in the images, the C filaments have an average diameter of 7  $\mu\text{m}$  thus any nanometric size impurity can affect their surface appearance.



a)



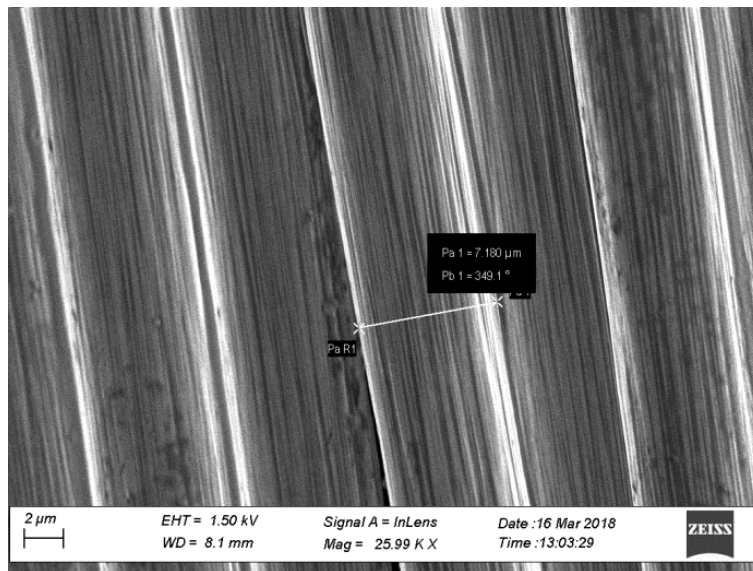
b)

Fig. 4-1: SEM images of as received carbon fibers. a) TENAX HTA 5131; b) TORAY FT300B

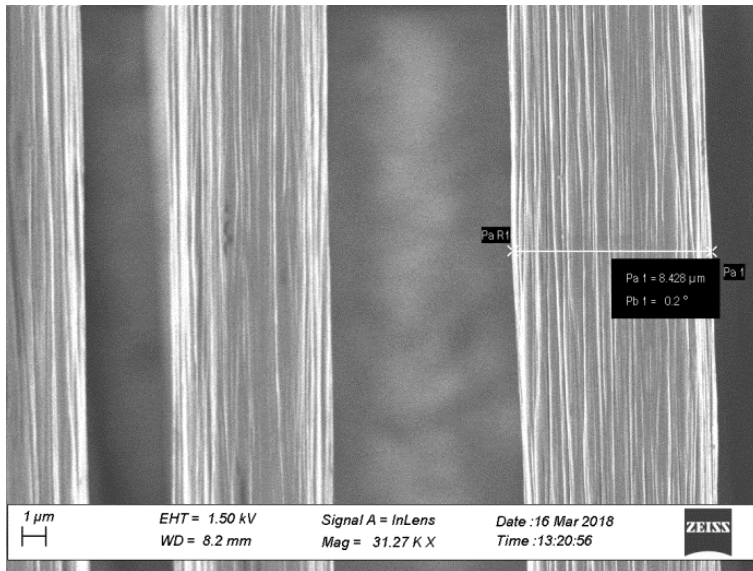
#### 4.1.2 SEM analysis after desizing

With the aim of verifying the effectiveness of the desizing process of the carbon fibers, direct SEM analysis was performed after the C yarns were extracted from the furnace. By using a magnitude of 30 KX it was possible to observe the effect of the heat treatment on the surface of the C filaments. As already explained in chapter 3, the temperature chosen for the treatment was 500 °C with 5, 60 and 120 minutes of time treatment.

The SEM images are reported below. Even with high levels of magnitude it is difficult to impeccably characterize the surface of the filaments. Indeed, as already mentioned in the previous chapter, the polymeric sizing is few nanometers thick and is not distributed uniformly on the surface. Furthermore, the manipulation and the conservation conditions of the fibers itself can bring micro impurities that affect observations. A clear example of impurities brought by the manipulation is shown in Fig. 4-3 a). The impurity has a spherical shape with an estimated diameter of around 2  $\mu\text{m}$  but its composition is unknown. The desizing through heating does not have the same effect on different type of fibers as the polymeric coating has different chemical composition. This latter aspect will be discussed more in depth in chapter 5.

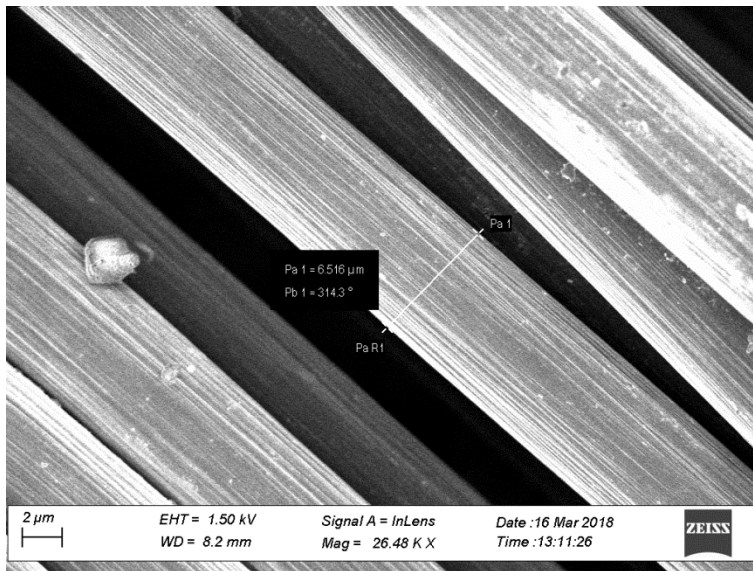


a)

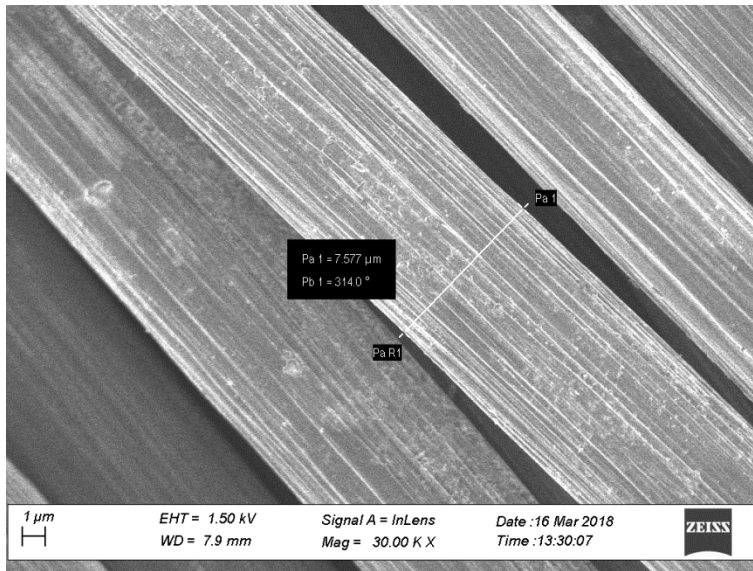


b)

Fig. 4-2: SEM images of carbon fibers after 5 min at 500 °C. a) TENAX HTA 5131; b) TORAY FT300B



a)



b)

Fig. 4-3: SEM images of carbon fibers after 60 min at 500 °C. a) TENAX HTA 5131; b) TORAY FT300B

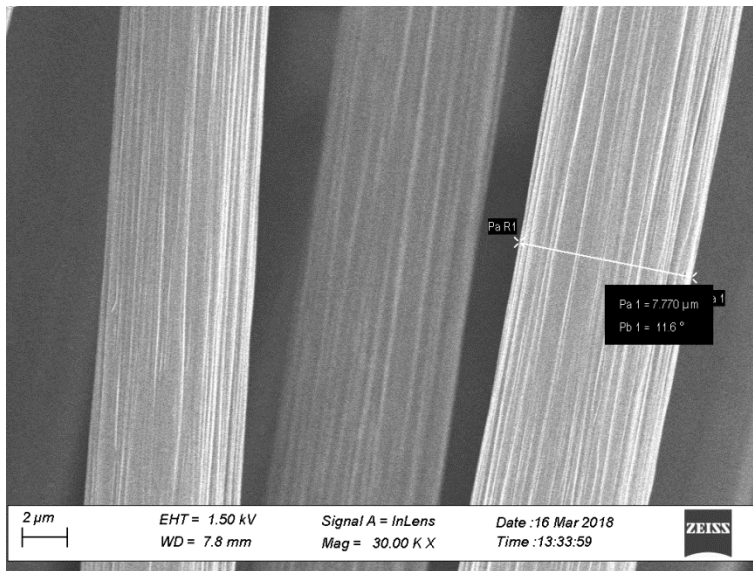


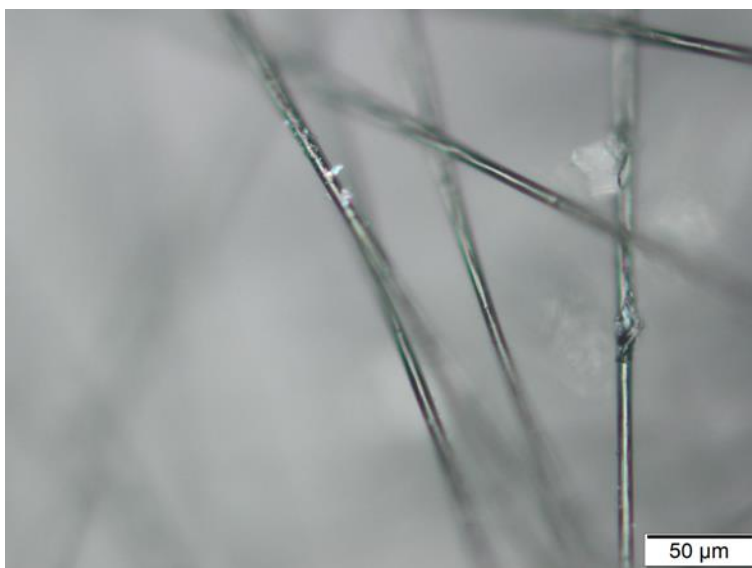
Fig. 4-4: SEM image of TORAY FT300B carbon fibers after 120 min at 500 °C.

## 4.2 $K_2ZrF_6$ TREATMENT RESULTS

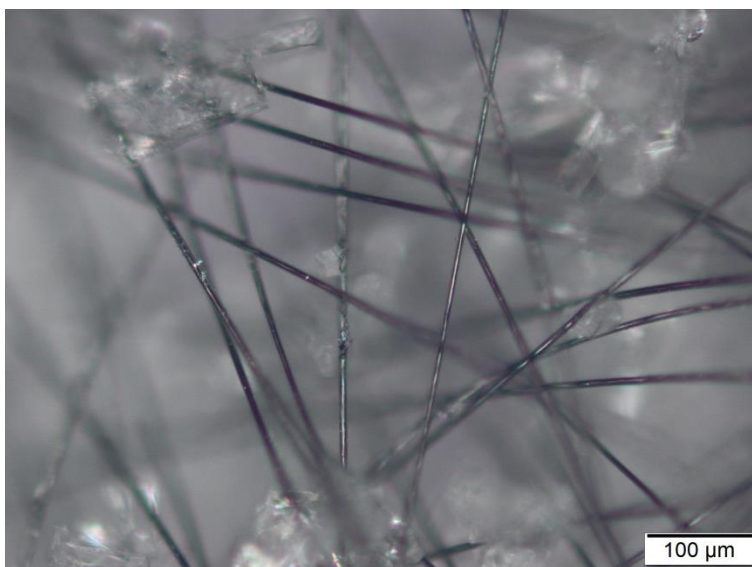
In this section will be reported the images obtained from the optical microscope as well as SEM observations of the carbon fibers after the  $K_2ZrF_6$  treatment. In the third chapter were exposed the different process parameters adopted for this treatment in order to optimize the process. The fundamentals aspects to be considered in this case are the size of the  $K_2ZrF_6$  crystals deposited on the carbon filaments along with the level of their regularity. Different level of magnification are used with both microscopes in order to have a general view of the appearance of the surface treated fibers as well as the micrometric characteristics of the  $K_2ZrF_6$  crystals deposited on the carbon filaments. It is worth noting that the observation of such filaments is complicated by the fact that it is not possible to place them in a flat coplanar surface. The treated filaments do not stay parallel between them and so the distance with the observing lens is different on the filament length causing often a lack in focus. Furthermore, it is not possible to stick the filaments in a sample support as this operation modifies the characteristics of the surface treatment and therefore compromises the observations. Optical microscope observations are the more influenced by those aspects and this therefore causes a poor focus on the crystals observations as it is shown in Fig. 4-5.

#### 4.2.1 Optical microscope images of treated fibers

The optical microscope images of the carbon filaments after the  $K_2ZrF_6$  treatment are shown below. As already mentioned, the level of focus is poor due to the misalignment of the carbon filaments which involve a variation of the distance with the microscope lens.



a)



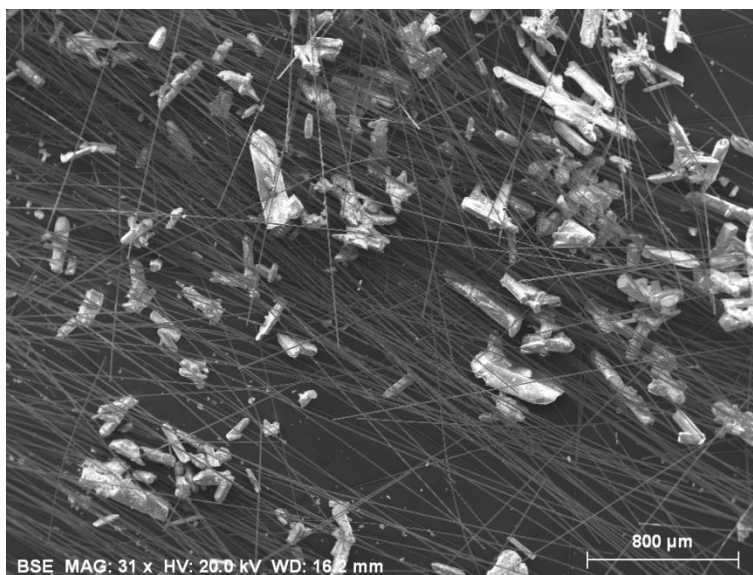
b)

*Fig. 4-5: images of  $K_2ZrF_6$  crystals observed on optical microscope. a) 20x magnification; b) 10x magnification.*

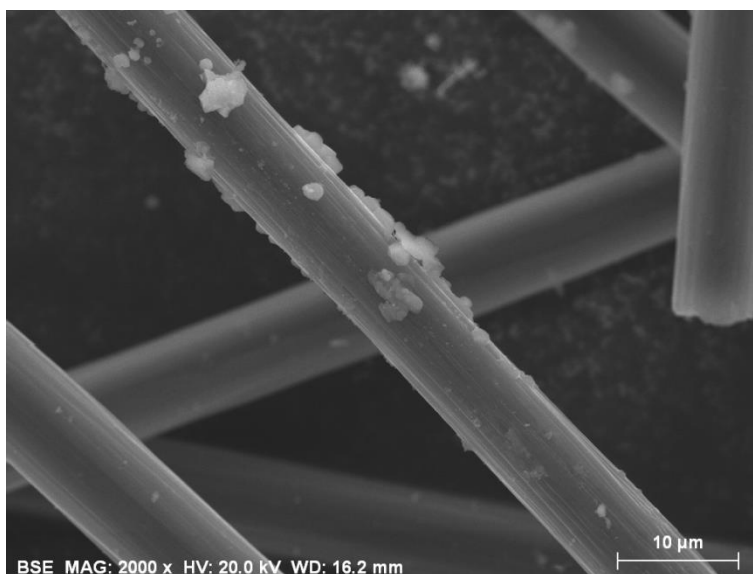
#### 4.2.2 Treated fibers surface SEM analysis results

Both of the carbon yarns have been observed using SEM in order to study the effect of the process parameters of the  $K_2ZrF_6$  treatment. Indeed, it is hypothesized that the  $K_2ZrF_6$  crystals distribution on the surface of the carbon filaments is influenced by the temperature as well as the dip-in time of the treatment. Moreover the level of the magnetic stirring adopted to maintain a homogeneous solution should be considered to affect the quality of the treatment. The effect of all of these parameters will be discussed in the next chapter. In this subsection are reported the SEM images of the carbon fibers treated using different process parameters. First are shown the SEM results of the same dip-in time treatment (2 minutes) performed at two different values of temperature (80 and 95 °C). Secondly, are shown the results of maintaining a steady value of temperature of 95 °C and changing the dip-in time (1 and 5 min).



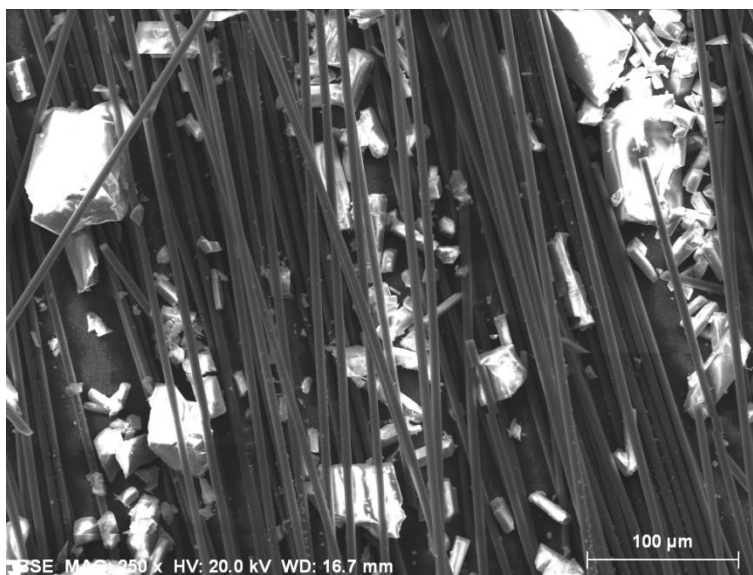


a)

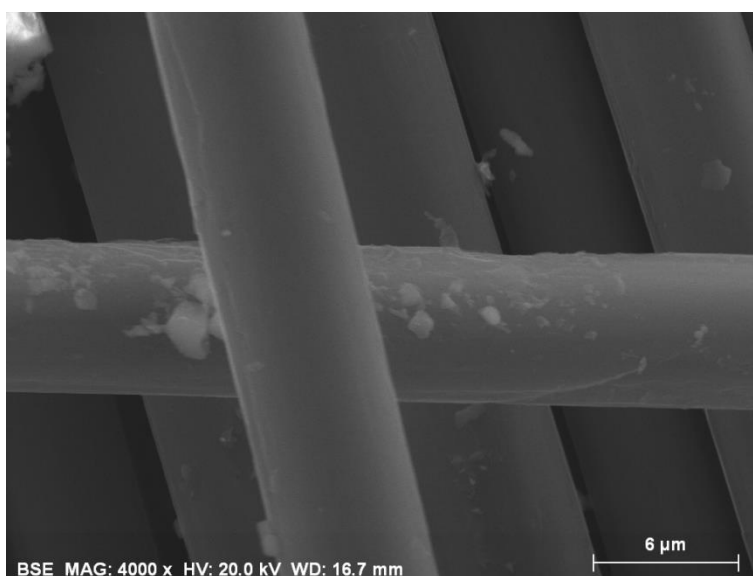


b)

*Fig. 4-6: SEM images of TORAY FT300B carbon fibers after  $K_2ZrF_6$  treatment for 2 min at 95 °C: a) 31x magnification; b) 2000x magnification.*

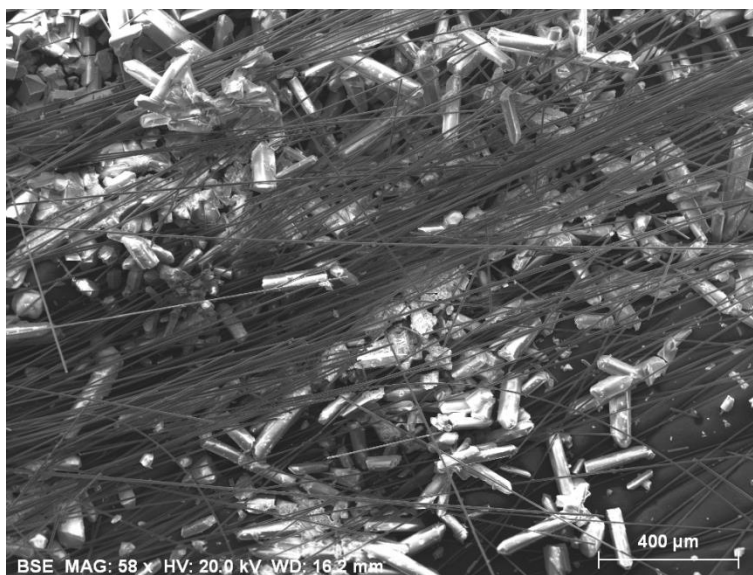


a)

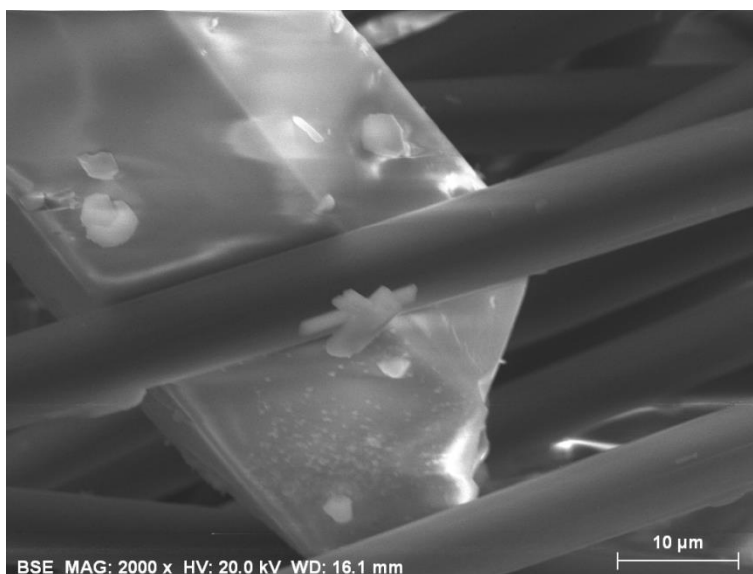


b)

*Fig. 4-7: SEM images of TENAX HTA 5131 carbon fibers after  $K_2ZrF_6$  treatment for 2 min at 95 °C. a) 250x magnification; b) 4000x magnification.*

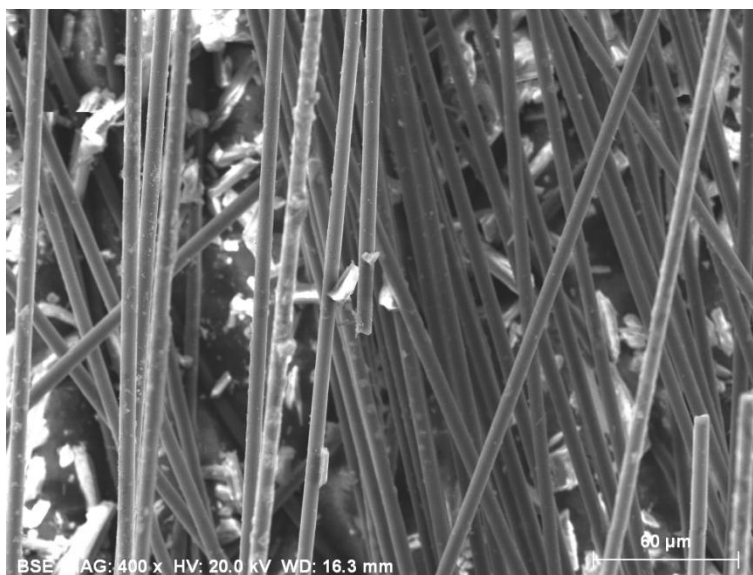


a)

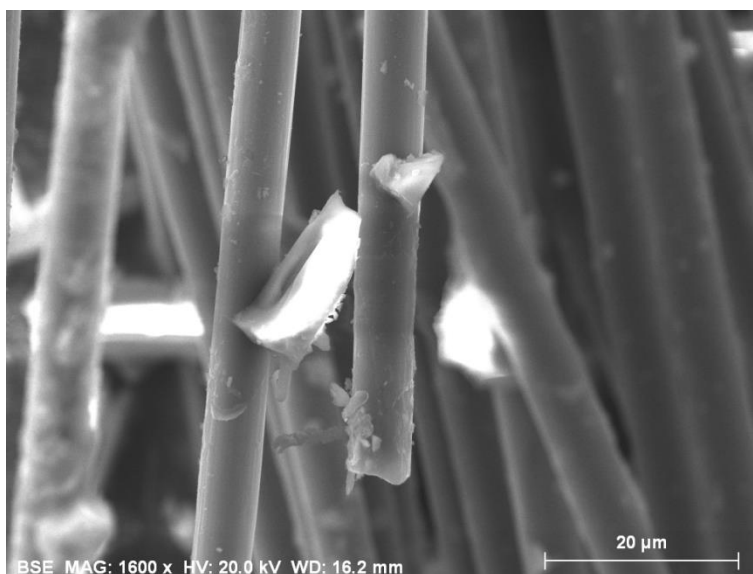


b)

*Fig. 4-8: SEM images of TORAY FT300B carbon fibers after  $K_2ZrF_6$  treatment for 2 min at 80 °C. a) 58x magnification; b) 2000x magnification.*

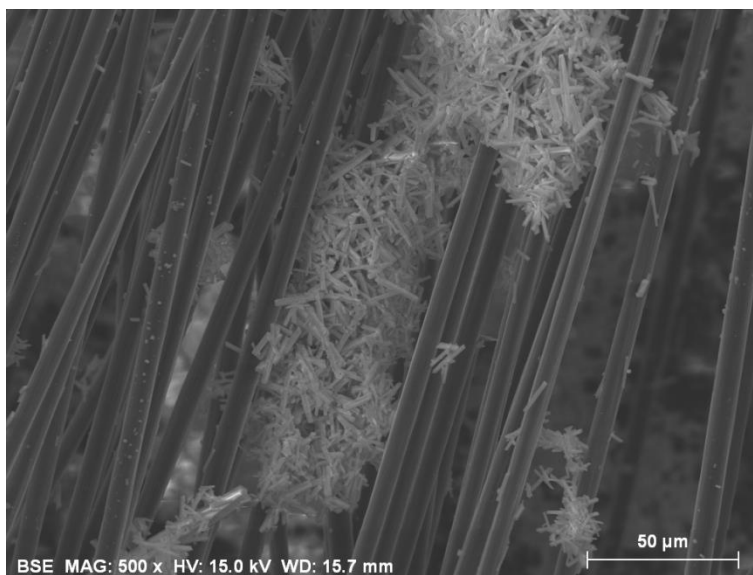


a)

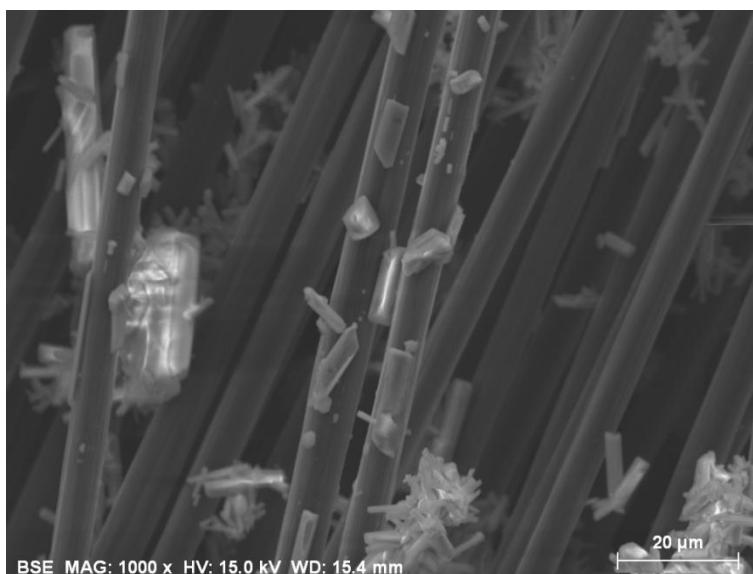


b)

*Fig. 4-9: SEM images of TENAX HTA 5131 carbon fibers after  $K_2ZrF_6$  treatment for 2 min at 80 °C. a) 400x magnification; b) 1600x magnification.*

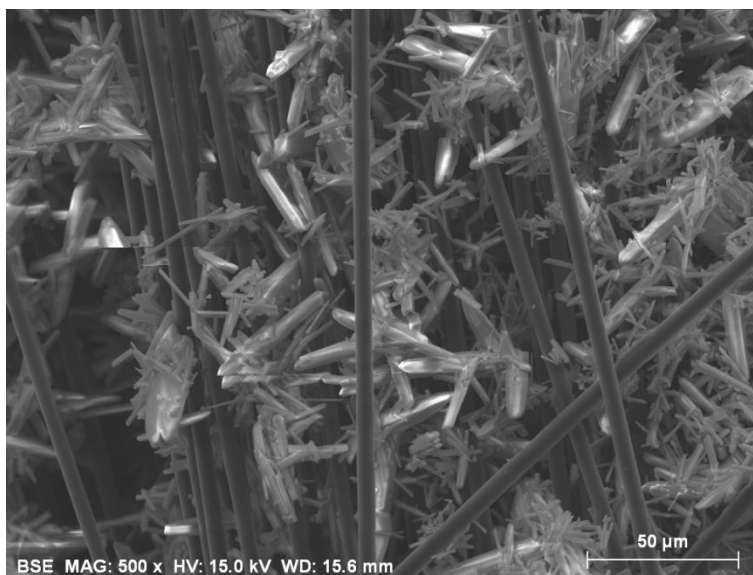


a)

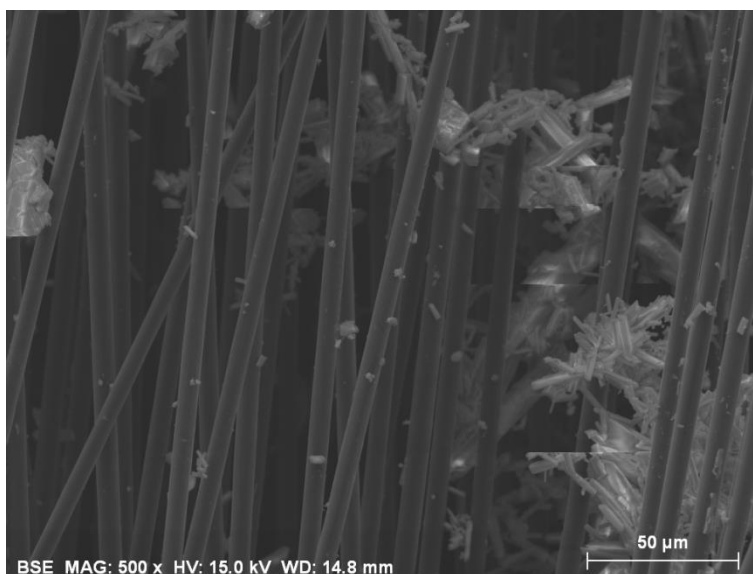


b)

*Fig. 4-10: SEM images of TORAY FT300B carbon fibers after  $K_2ZrF_6$  treatment at 95 °C: a) for 1 min; b) for 5 min.*



a)



b)

*Fig. 4-11: SEM images of TENAX HTA 5131 carbon fibers after  $K_2ZrF_6$  treatment at  $95^\circ\text{C}$ :  
a) for 1 min; b) for 5 min.*

### 4.3 THERMAL ANALYSIS RESULTS

DTA tests were executed to identify the exact melting curve of the commercial pure aluminum used in this work. Several DSC tests were performed in order to study the sequence of reactions occurring during the interface formation between surface treated carbon filaments and the metal matrix. In all the thermal diagrams reported in this work, the endothermic peaks are shown with up direction in the y-axis. Therefore all the peaks representing decomposition, destabilization as well as fusion will have peaks directed up in the vertical axis. On the contrary, the chemical reactions caused by the crystals of  $K_2ZrF_6$  deposited on the surface treated fibers are supposed to be exothermic, thus having down direction on the vertical axis. It is worth noting that the adopted representation method is valid both for heating and cooling spectra.

### 4.3.1 DSC spectra

First, DSC test of the aluminum that will be used to realize the C/Al composite was performed in order to verify its purity and to compare the heating and cooling spectra with the provided standard spectra of high purity aluminum. The measurement was executed using a heating rate of 5K/min starting from room temperature until it was reached the final temperature of 750°C then maintained for 1 min. Finally it was embraced a cooling rate - 5K/min for bringing the sample back to the value of room temperature. Unless it's not explicitly indicated, these specified are the same parameters adopted in any of the performed measurements.

The results are plotted in the following spectra only in the specific range of interest.

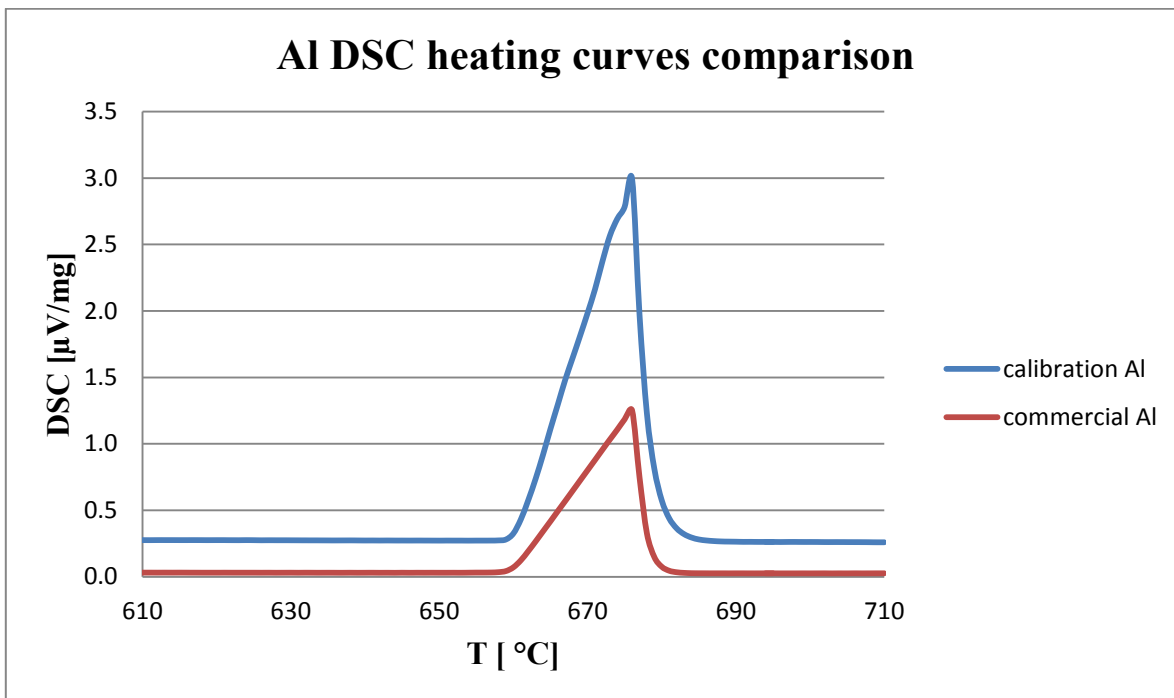


Fig. 4-12: DSC heating curves comparison between calibration and commercial pure Al.



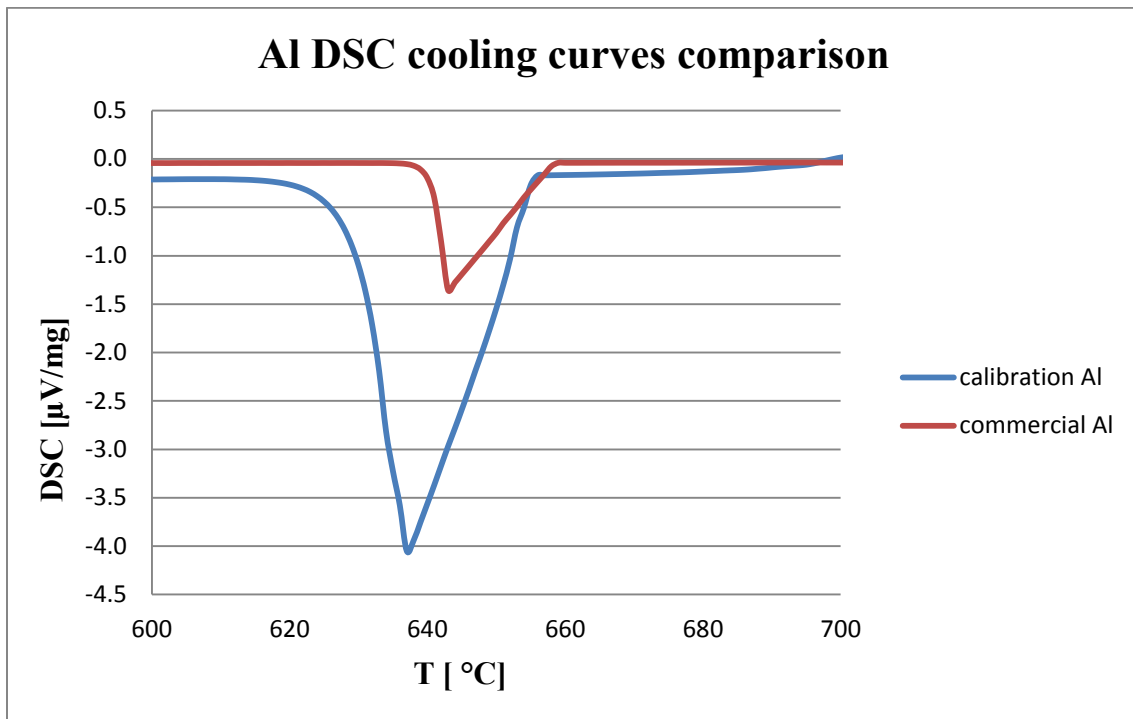


Fig. 4-13: DSC cooling curves comparison between calibration and commercial pure Al.

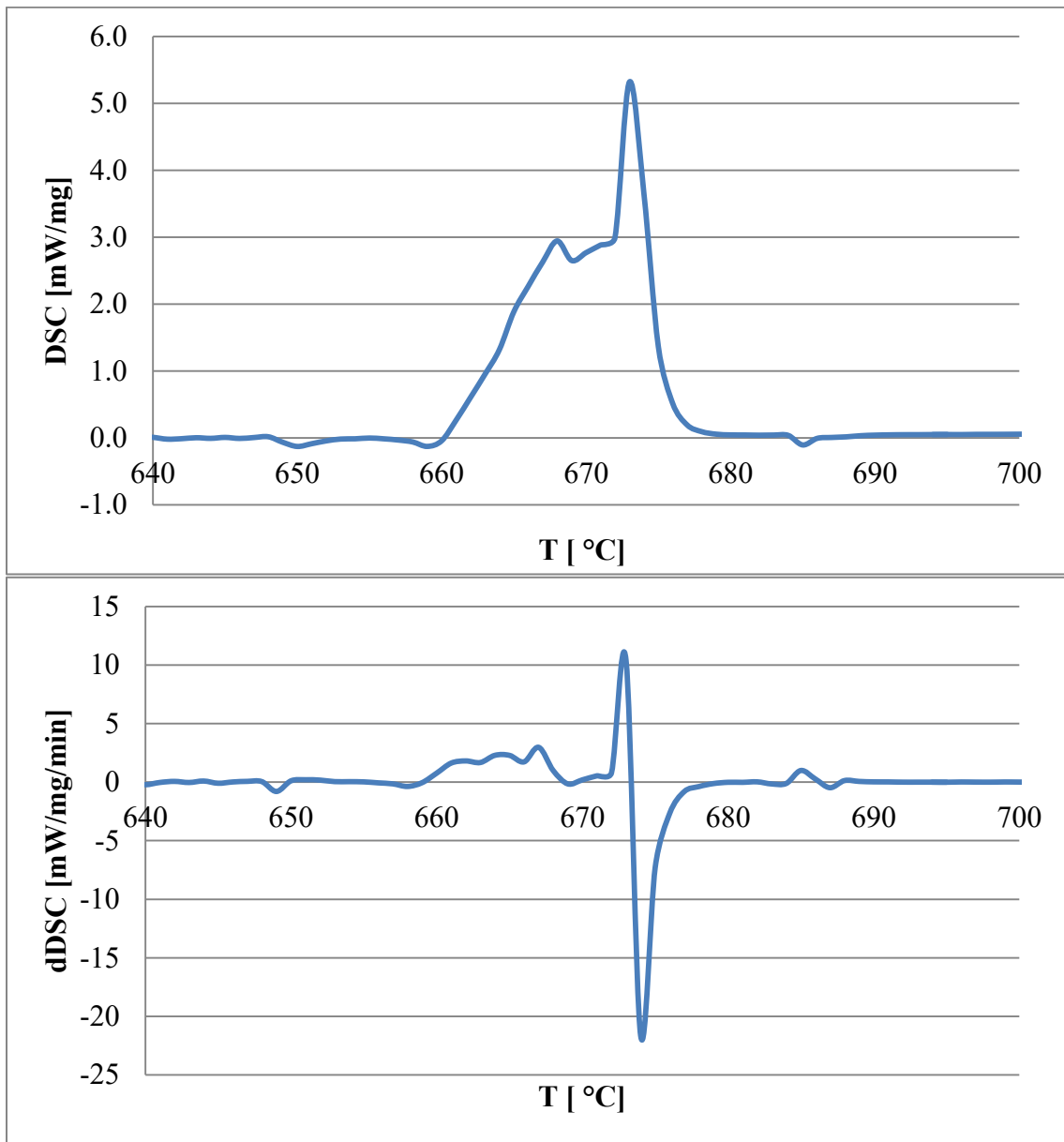


Fig. 4- 14: DSC spectra and first derivative heating curve of composite sample with TORAY FT300B fibers  $\text{K}_2\text{ZrF}_6$  treated at 95  $^{\circ}\text{C}$  for 2min.

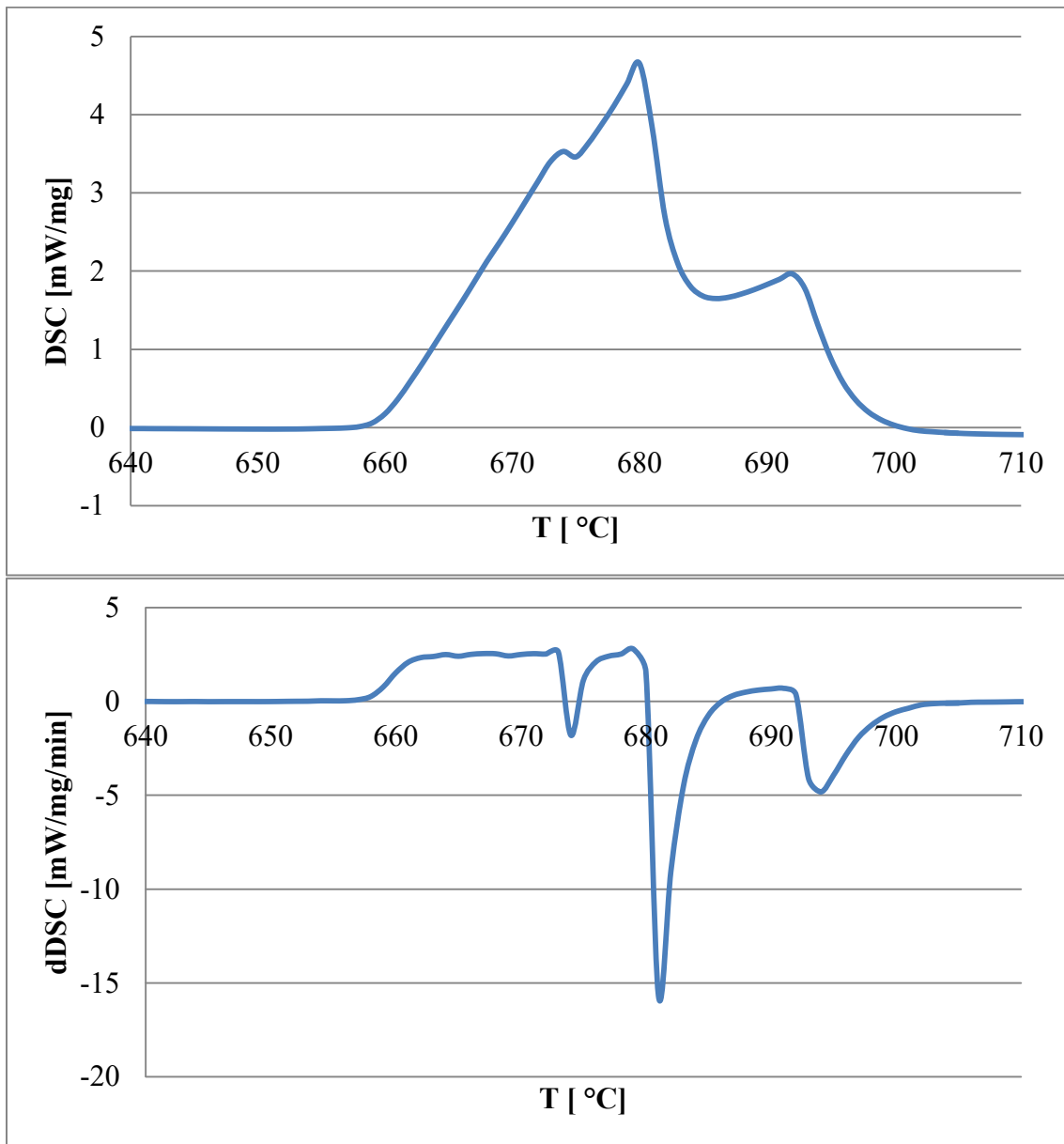


Fig. 4-15: DSC spectra and first derivative heating curve of composite sample with TENAX HTA 5131 fibers  $\text{K}_2\text{ZrF}_6$  treated at 95  $^{\circ}\text{C}$  for 2min.

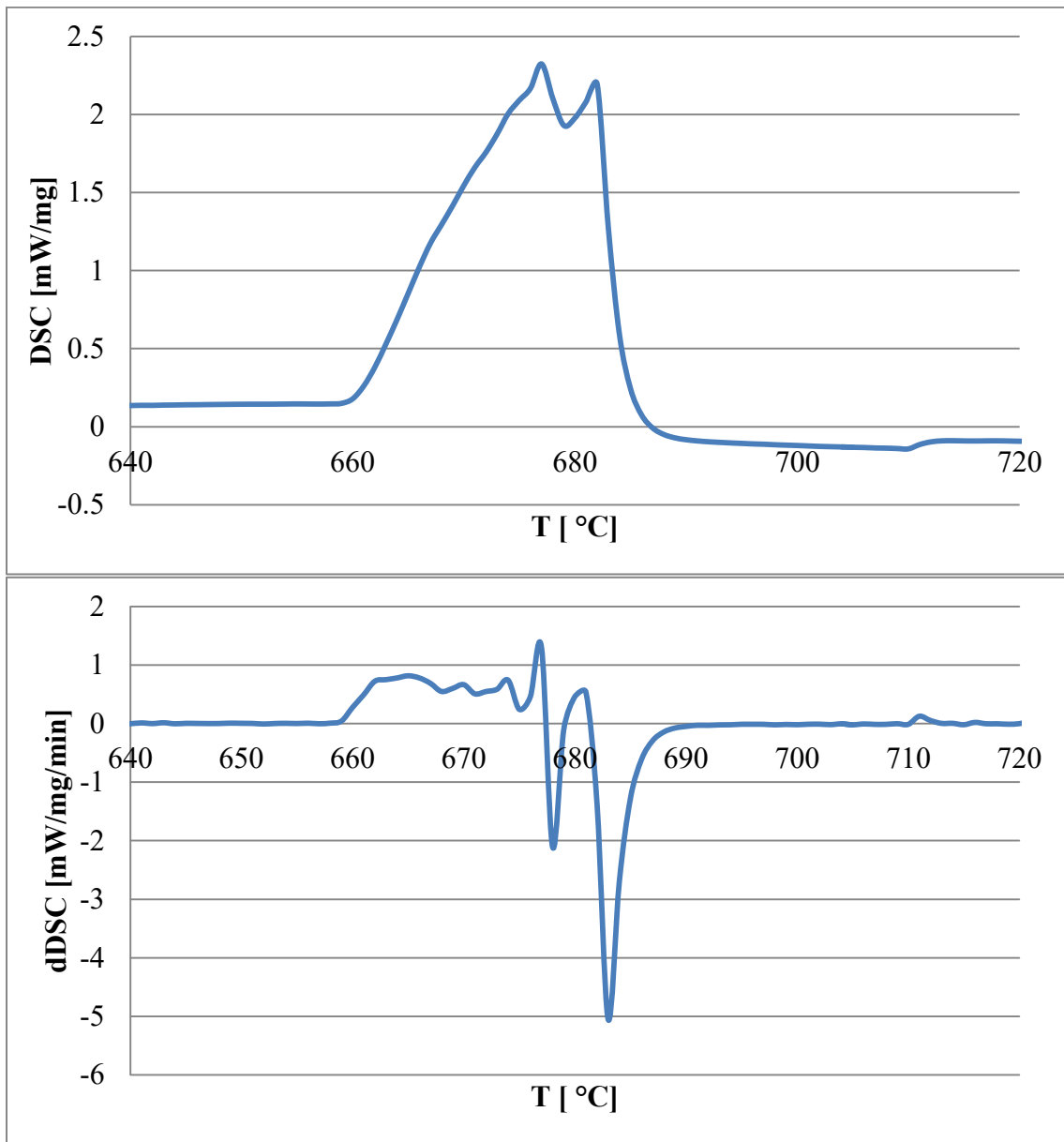


Fig. 4-16: DSC spectra and first derivative heating curve of composite sample with TORAY FT300B fibers  $\text{K}_2\text{ZrF}_6$  treated at  $80^{\circ}\text{C}$  for 2min.

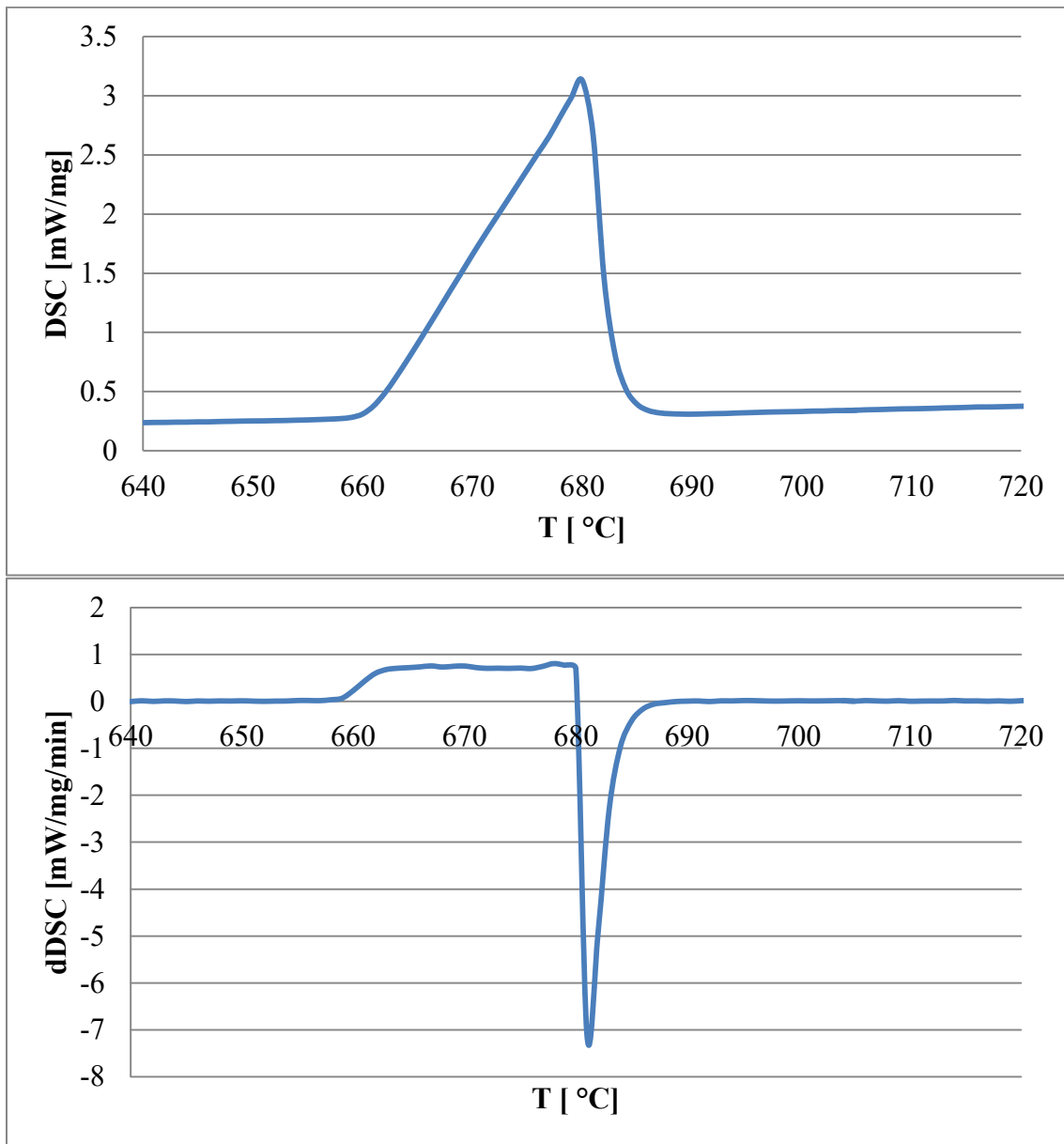


Fig. 4- 17: DSC spectra and first derivative heating curve of composite sample with TENAX HTA 5131 fibers  $\text{K}_2\text{ZrF}_6$  treated at 80  $^{\circ}\text{C}$  for 2min.

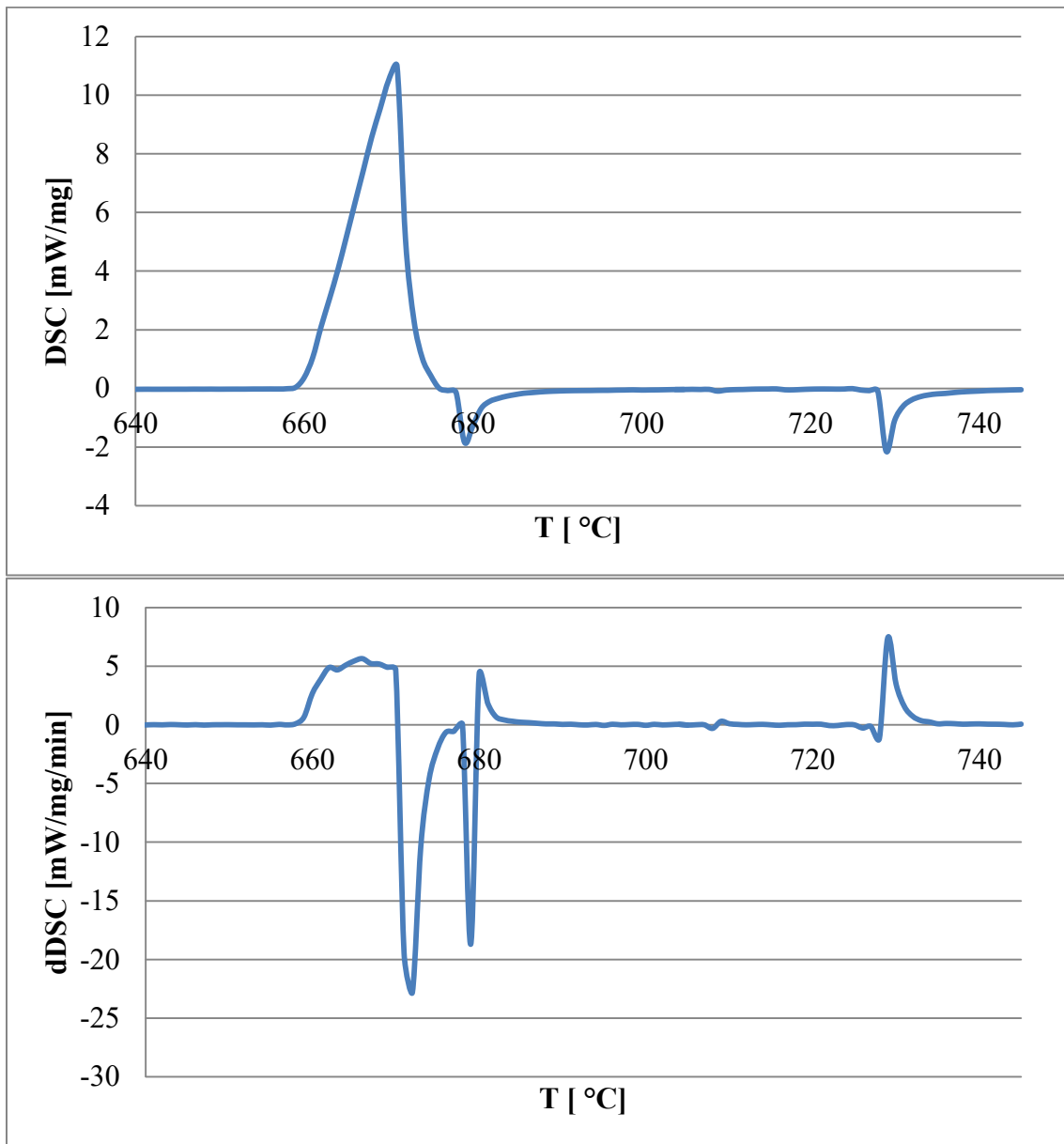


Fig. 4-18: DSC spectra and first derivative heating curve of composite sample with TORAY FT300B fibers  $K_2ZrF_6$  treated at 95 °C for 5 min.

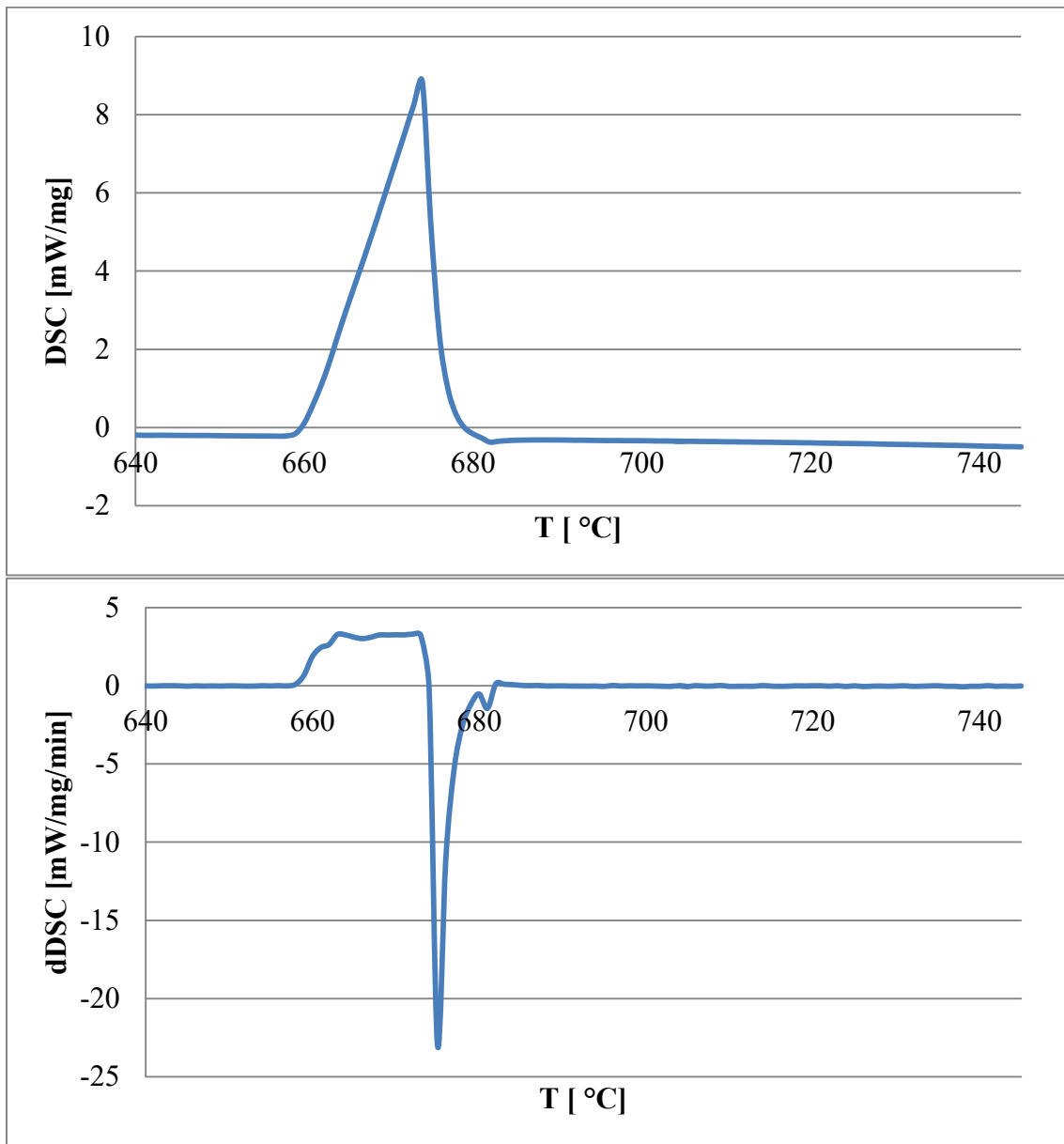
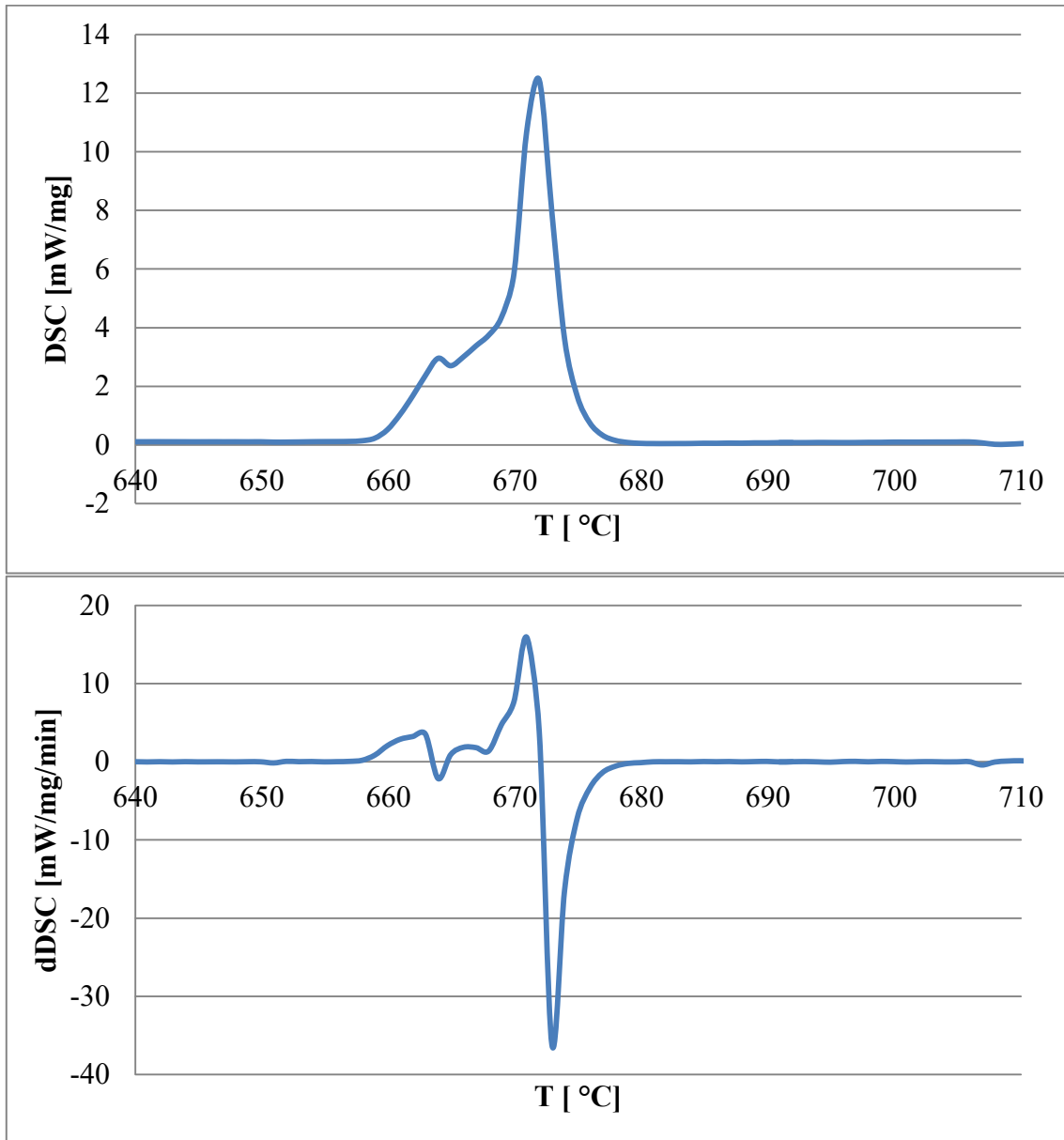


Fig. 4-19: DSC spectra and first derivative heating curve of composite sample with TENAX HTA 5131 fibers  $K_2ZrF_6$  treated at 95 °C for 5 min.

After several  $K_2ZrF_6$  treatments, the best results seemed to be obtained using TORAY FT300B fibers treated at  $95\text{ }^\circ\text{C}$  for 5 min. In order to study any differences on the sample characteristics caused by the DSC test parameters, DSC test with final temperature of  $800\text{ }^\circ\text{C}$  and heating rate of  $5\text{ }^\circ\text{C}/\text{min}$  was performed to realize 3 samples. The most noteworthy DSC curve and its first derivative diagrams are shown below.



*Fig. 4-20: DSC spectra and first derivative heating curve of composite sample with TORAY FT300B fibers  $K_2ZrF_6$  treated at  $95\text{ }^\circ\text{C}$  for 5 min. In this case the DSC final temperature was  $800\text{ }^\circ\text{C}$  and the heating rate was  $5\text{ }^\circ\text{C}/\text{min}$ .*



#### 4.4 COMPOSITE SAMPLE MICROSTRUCTURE

The small composite samples obtained from the DSC test were first observed using SEM in order to characterize the level of wettability enhancement brought about by the surface treatment performed on the C fibers. Secondly, the samples were mounted and polished with the aim of allowing direct SEM observations of the interface between the aluminum matrix and the treated C fibers. However, the fibers were not deposited uniformly and that made it difficult to have an optimal cross section to observe. In this section will be shown the optical microscope images of the mounted and polished samples as well as the SEM images of composite samples before and after polishing.

##### 4.4.1 Composite sample optical microscope images

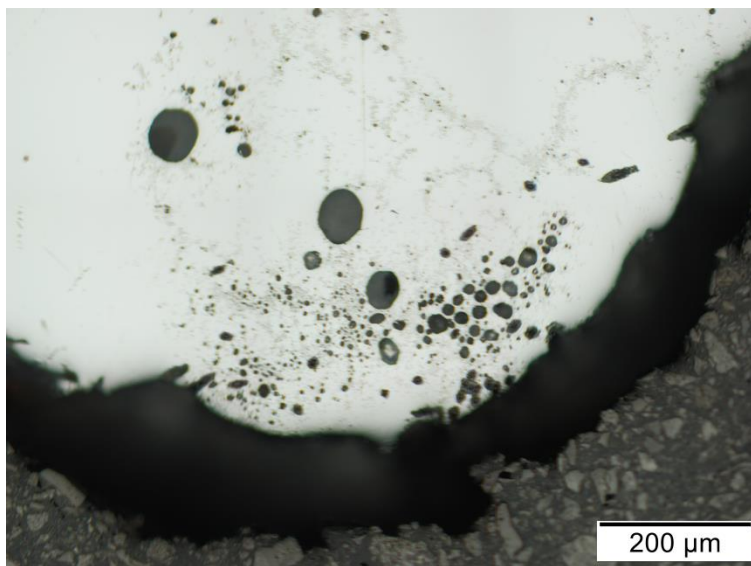


*Fig. 4-21: optical microscope image of the mounted and polished composite sample.*

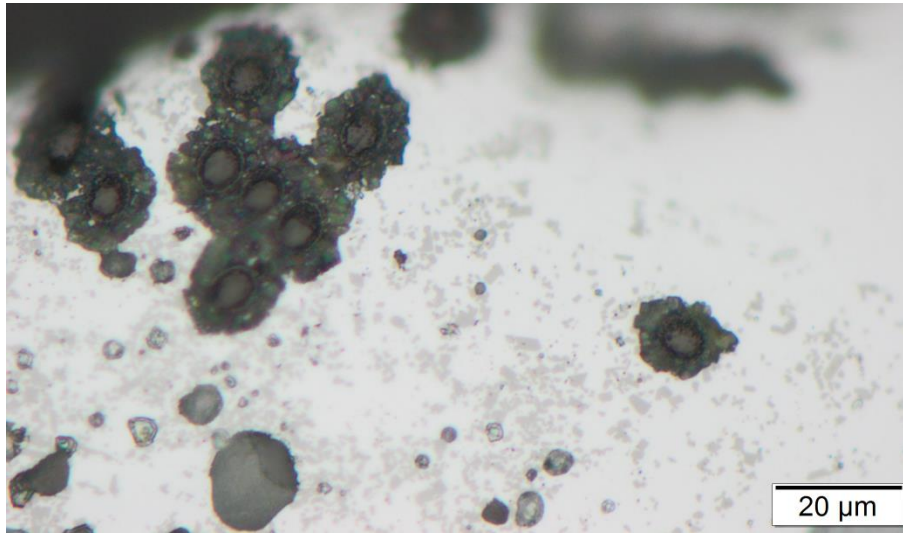


*Fig. 4-22: zoom on the fibers concertation area.*

#### **4.4.2 Composite SEM analysis results**

In this subsection will be reported the SEM images of the composite samples before and after being subjected to the procedure of mounting and polishing. Furthermore, chemical composition spectra will be reported for some of the samples.

The following image refers to the composite sample as received from DSC test. The carbon fibers in this case were treated at 95°C for 2 min in supersaturated solution.



*Fig. 4-23: General sample observation of the unmounted sample.*

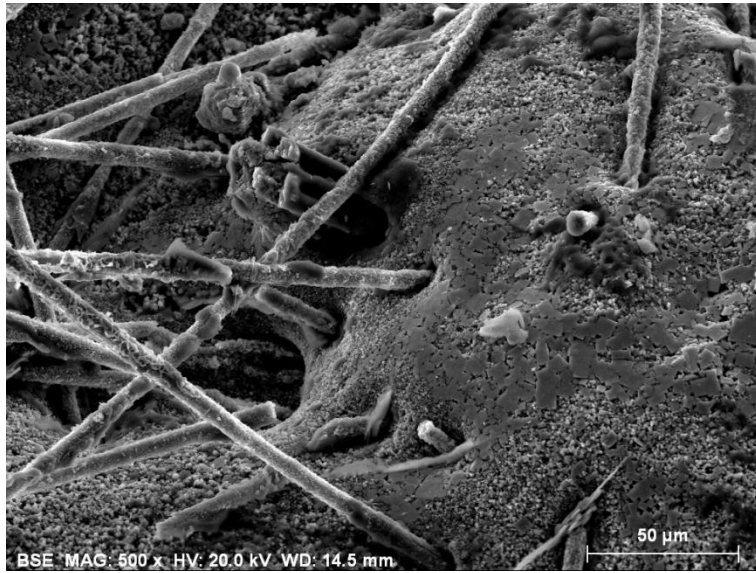


*Fig. 4-24: carbon fibers embedded on the matrix.*

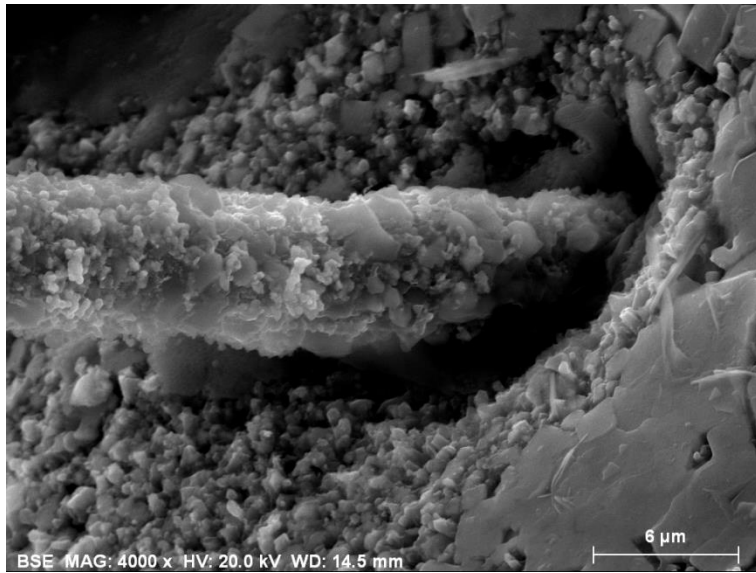


*Fig. 4-25: carbon fibers covered by K<sub>2</sub>ZrF<sub>6</sub>.*

After mounting and polishing the sample, SEM observations helped in understanding the characteristics of the sample. From a first view, as expected, it is possible to notice the non-homogeneity of the sample: there are areas with fibers concentration while some others appear to be composed by aluminum matrix only. Different holes and craters are detected on the sample, probably also due to the polishing process.

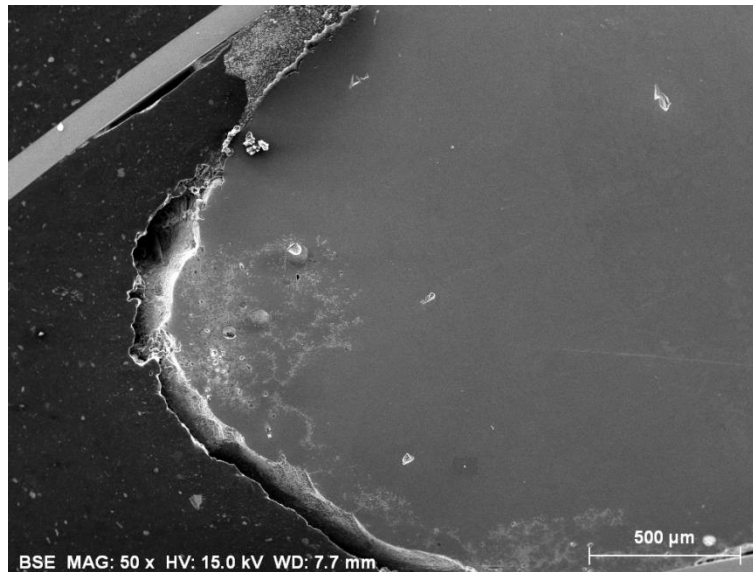


*Fig. 4-26: polished sample general SEM view.*

By zooming in the interested area containing the carbon filaments, the resulting SEM image is showed in Fig. 4-27.

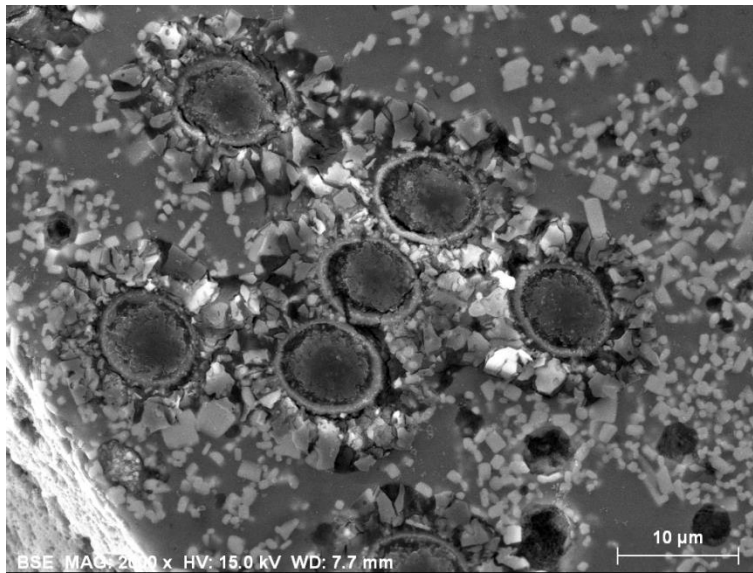


*Fig. 4-27: polished sample carbon fibers concentration area.*

The fibers are clearly visible from this image but it is worth noting the high discontinuity of the phases in the sample.

At the interface between the fibers and the matrix, there is a first regular layer in contact with the carbon fibers followed by different layers where the microstructure appears irregular. However it is possible to state that there is a good impregnation of the carbon filaments from the molten aluminum and so it seems that the adopted K<sub>2</sub>ZrF<sub>6</sub> treatment worked properly in improving the wettability of the carbon filaments by molten Al. However, the presence of high amount of unreacted K<sub>2</sub>ZrF<sub>6</sub> is detected on the image with the typical white crystals of different size and shape meaning that the quantity of deposited K<sub>2</sub>ZrF<sub>6</sub> crystals on the fibers was superior to the one needed for the spontaneous favoring of carbon filaments wetting.

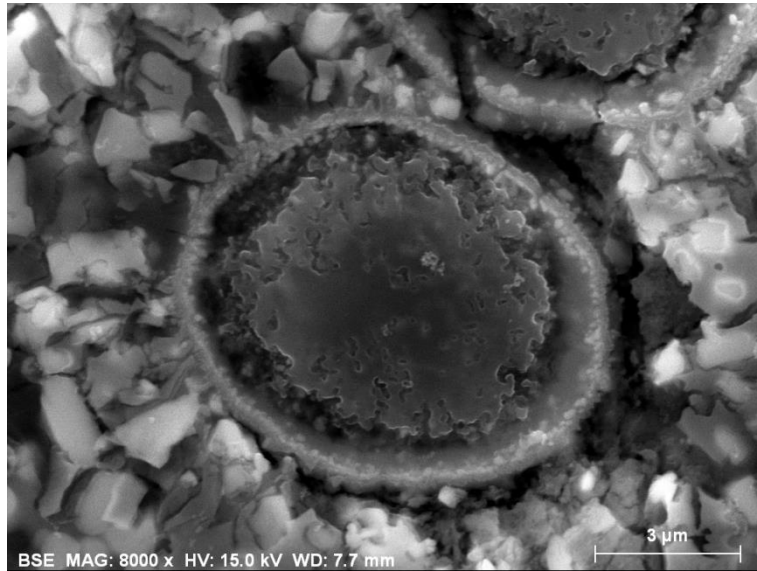


*Fig. 4-28: Interface observation between surface treated C filament and the Al matrix.*

The above image makes it possible to see the damage occurred on the C fibers. In fact, on the external diameter, it can be noticed a consumption of carbon probably due to the strong reaction between the pretreated C fibers and the Al matrix. Some cracks are also visible at the external zone of the interface.

After performing the DSC test with final temperature of 800°C and heating rate of 5°C/min the 3 samples were mounted and polished with the same parameters of the previous samples. The resulting SEM images and EDS spectra are shown below.

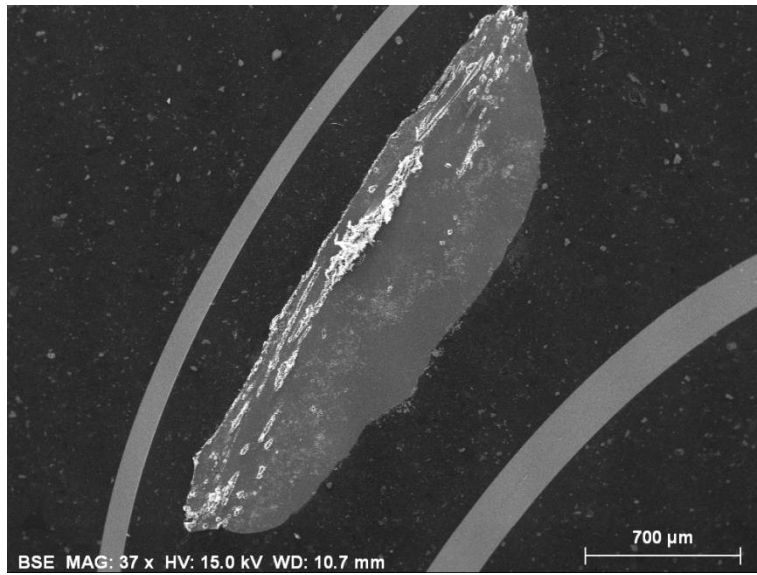


*Fig. 4-29: mounted and polished sample A general SEM view.*

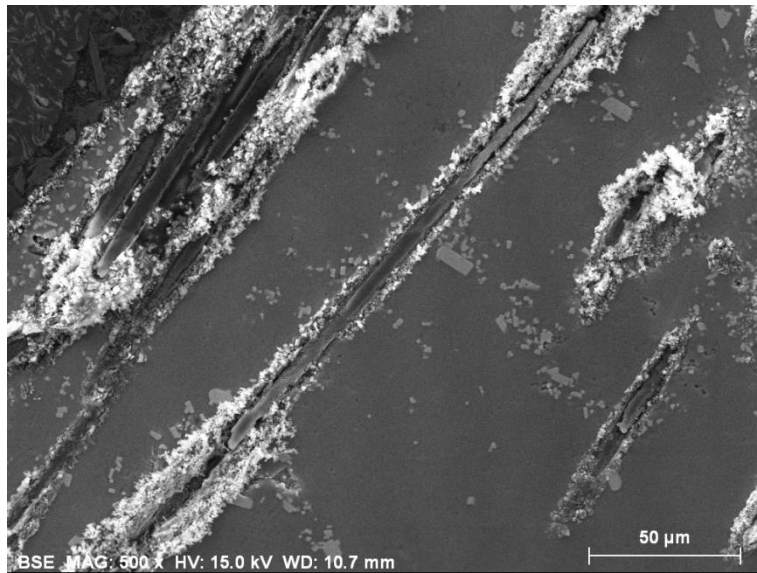


*Fig. 4-30: horizontal exposed fibers embedded in the matrix of sample A.*

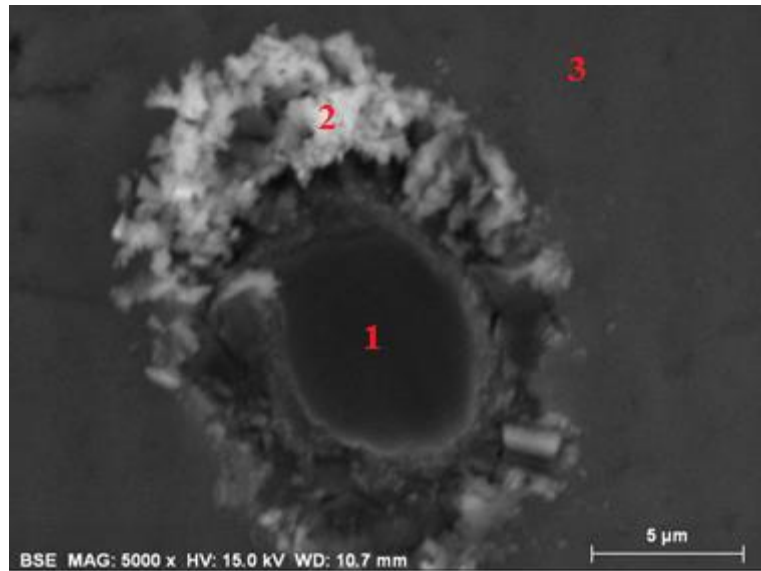
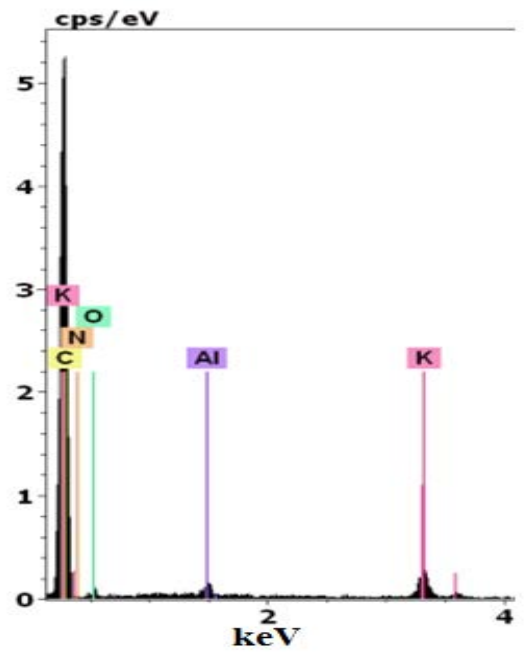
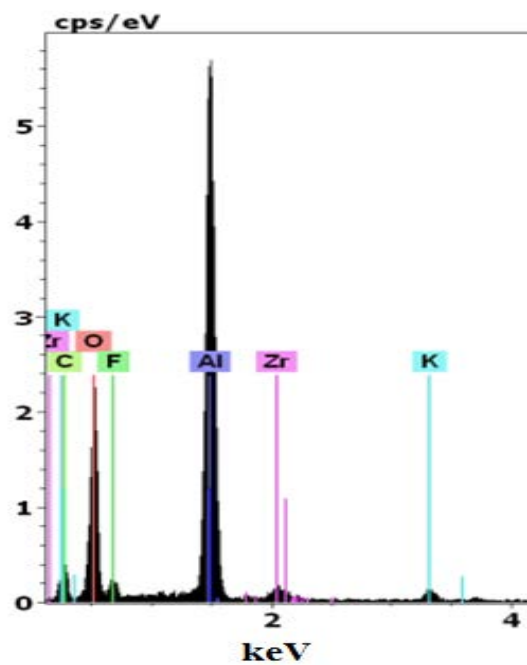


Fig. 4-31: 5000x magnification on fiber-metal interface of sample A. The numbers in red indicate the points where EDS was performed.

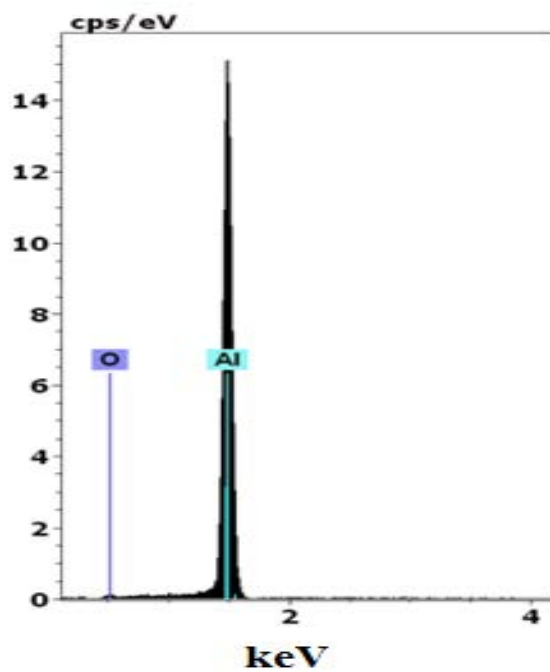


1)





2)



3)

Fig. 4-32: EDS results of the fiber-metal interface shown in fig 4-31. The indicated numbers 1, 2, 3 correspond to the ones of Fig. 4-31 points.

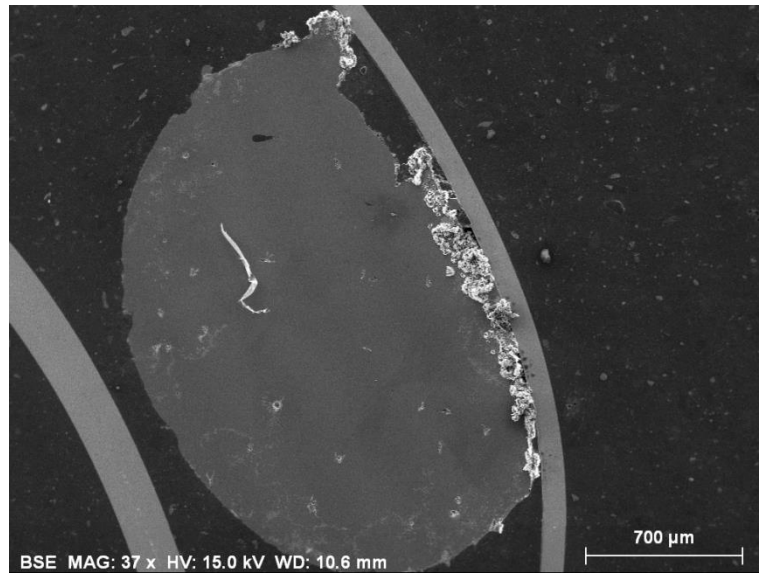


*Fig. 4-33: mounted and polished sample B general SEM view.*

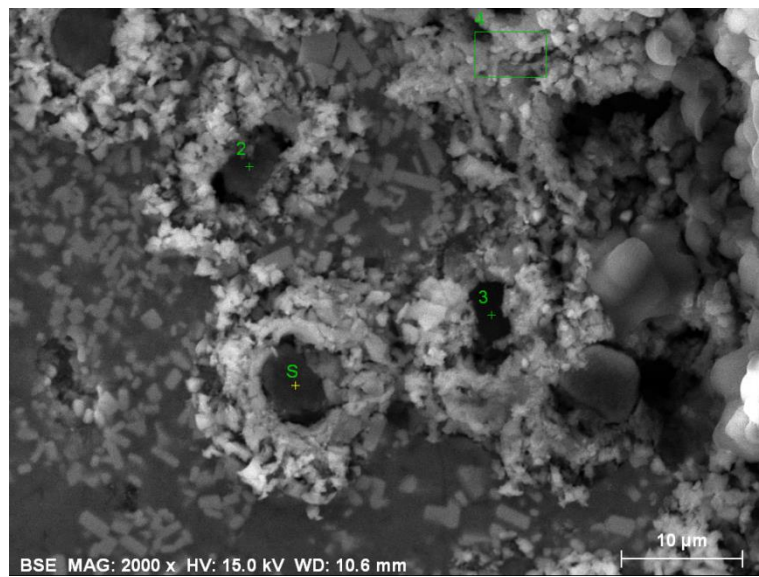


*Fig. 4-34: exposed fibers of sample B with white  $K_2ZrF_6$  crystals.*

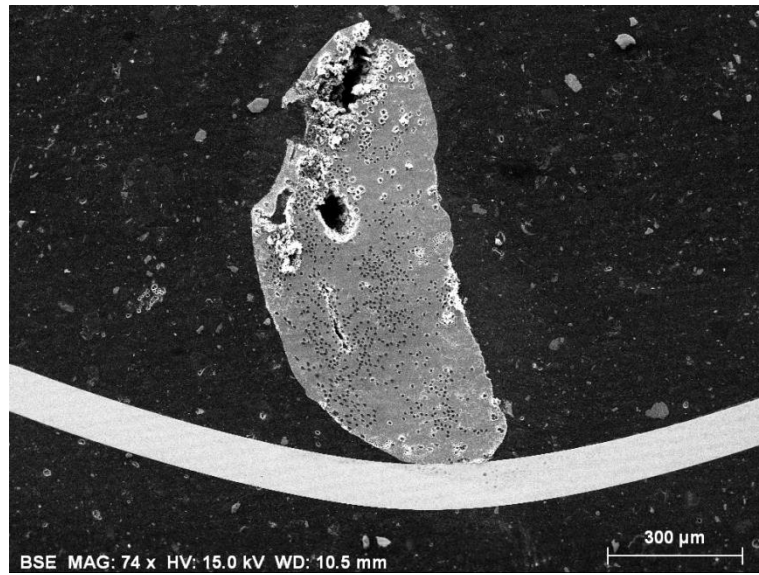


*Fig. 4-35: mounted and polished sample C general SEM view.*

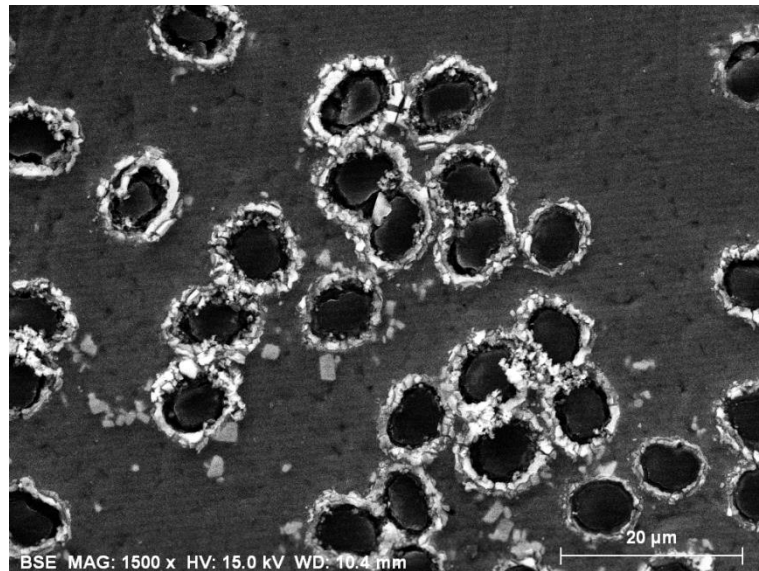


*Fig. 4-36: zoom at 1500x magnification on sample C at the good infiltration zone.*

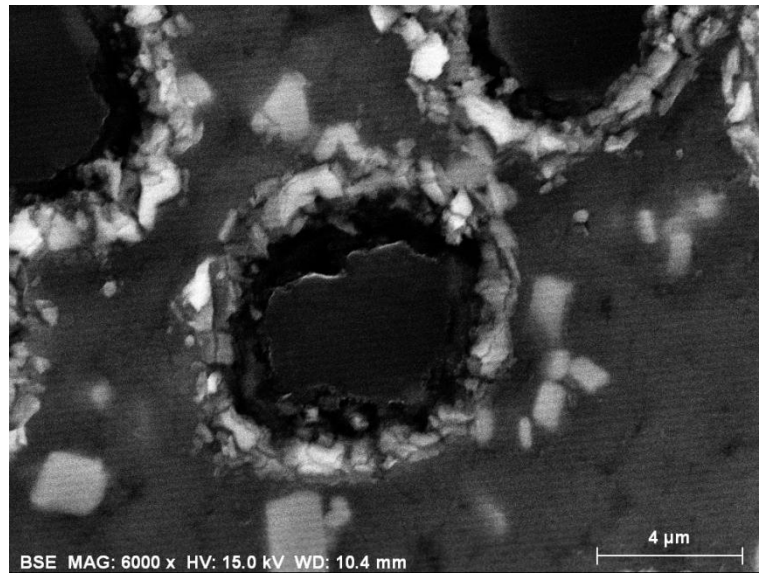


*Fig. 4-37: sample C: interface fiber-metal at 6000x magnification.*

## 5. DISCUSSION

This chapter discusses the results obtained and presented in the previous chapter. First, it will be discussed the influence of desizing and  $K_2ZrF_6$  process parameters on the carbon fibers. Secondly, the characteristics of the  $K_2ZrF_6$  treatment will be analyzed also regarding the interface formation. Finally, it will be discussed the final microstructure of the composite samples.

### 5.1 CARBON FIBERS SURFACE

The main part of the experimental work consisted in the surface treatment of the carbon fibers. The first part of the experimental work consisted in the desizing process that was followed by the aqueous solution treatment with  $K_2ZrF_6$ . The following discussion focuses precisely on these aspects, highlighting the most significant results and pinpointing the encountered difficulties.

#### 5.1.1 Desizing considerations

The commercially available carbon fibers are, as already mentioned, coated by a sizing layer on the surface, which usually is either a solution or emulsion consisting of polymeric components. Sizing is supposed to improve inter-filamentary adhesion and aid in wetting out the fiber in resin matrices. However, this sizing layer is undesired when the fibers are used to produce metal matrix composites. Indeed, the molten metal coming in contact with the fibers cause an evaporation of the polymeric coating that could give rise to gas phase formation that can generate porosity in the fiber-metal interface. Nowadays we are assisting to a growing spread of carbon reinforced metal matrix composites and the carbon fibers producers are bringing on the market a large choice of unsized fibers and specifically designed for MMCs. Notwithstanding this fact, part of this work consisted on studying the various desizing processes suggested in literature and picking up the most convenient one and testing it on the as received carbon yarns. The tested desizing process simply consisted in heating up the carbon yarns to a sufficient level of temperature for the minimum time

possible by making use of a furnace with air circulation. It was found out that the temperature needed to evaporate the polymeric layer covering the carbon filaments was 500°C which had to be maintained for 2 hours. Several difficulties in manipulating the fibers after the desizing are brought about by the fact that the filaments tend to fall apart. From this point on, the handling of the carbon yarns represents also a possible contamination of the filaments by small impurities. A clear example of this fact was shown on *Fig. 4-3 a)*, where a spherical shape impurity was detected on the filaments using scanning electron microscopy (SEM). Despite SEM analysis provide a good estimation of the desizing efficiency, in literature it is suggested to use Fourier Transform Infrared Spectroscopy (FTIR) in ATR MODE for a better result.

### **5.1.2 Characteristics of $K_2ZrF_6$ treatment**

The  $K_2ZrF_6$  pretreatment on carbon fibers has been quite intensively studied as it is thought to be one of the most economical solutions in producing light alloys reinforced with carbon fibers, mainly using aluminum alloys and magnesium as matrix. However, most of the issues that were discovered in the first studies decades ago still need to be solved. One of the main problems relies on the process parameters of the treatment. Indeed, the  $K_2ZrF_6$  salt has a strongly irregular degree of solubility in water and the main parameter that controls the characteristics of the treatment is the temperature of the solution. By taking a look of the solubility curve of  $K_2ZrF_6$  in water (*Fig. 2-2*) it is immediately clear that at low values of temperature, the salt barely dissolve in water. It can be stated that, for values of temperature lower than 40 °C, the degree of solubility of the salt is so low that it is expected to not have any appreciable deposition of  $K_2ZrF_6$  crystals on the carbon fibers regardless of the other process parameters. For values of temperature between 60 °C and 80°C the slope of the solubility curve begin to show significant increase confirming that the solubility is not linearly dependent on the temperature. Indeed, this aspect can be clearly noted in the range between 80 °C and 100 °C, where the slope of the curve strongly increase with small variations of temperature. In this range the solubility of the salt is high

but very unstable and this makes it very difficult to indirectly control the crystals deposition on the carbon fibers. In fact, a small variation of the system conditions, as it happens during the fibers dip-in phase, cause a variation of the temperature that bring to a change of the solubility which lastly influence the crystals deposition. In this work, the treatments were performed with large amount of solution in order to have a level of temperature as steady as possible during the dip-in process of the fibers. The reason for this choice relies on the fact that larger quantity of solution implies a higher thermal inertia. Thus the temperature do not varies so rapidly during the process lasting few minutes. However, it is suggested to adopted different thermal insulation systems so as to better control the temperature during the treatment. The more isothermal the solution is kept during the dip-in time, the higher the control of the solubility and so the higher the control of the crystals deposition on the carbon filaments can be obtained.

Another parameter that influences the characteristics of the treatment is the level of stirring of the solution. At low values of temperature and with low value of salt concentration, this parameter does not have any particular influence. However, when dealing with high concentrations, such as supersaturated solutions, the stirring becomes important as it controls the level of homogeneity of the solution. The latter affects not only the degree of uniformity of the crystals deposition on the carbon fibers but also the size of the  $K_2ZrF_6$  crystals itself. Indeed, when subjected to mixing, the non-dissolved salt that normally tents to precipitate on the bottom of the beaker, begin to float in the solution in a more homogeneous way as the stirring speed is increased. This implicates a higher degree of crystals that can meet the carbon filaments and deposit on them. Moreover, the stirring of the solution generates rotational mechanical forces that make the carbon fibers to align to the current directions. This fact causes a higher concentration of  $K_2ZrF_6$  crystals deposited on the external filaments of the carbon yarns and the size of the crystals itself is influenced by the stirring. Indeed, at high values of stirring, the mechanical forces of the rotation of the solution, do not allow to the crystals to grow in time causing a large amount of small crystals on the external carbon filaments. However, when the fibers are extracted from the beaker, the solution in excess that drop trough the filaments increases considerably the size deposition of crystals because the high concentration of small crystals already stacked on

filaments act as a catalyst for crystal growth once the mechanical force is removed. This makes it necessary to manually shake the fibers in order to reduce the size and the excessive quantity of crystals deposited on the external filaments of the carbon yarns. This phenomenon is even more evident when the treatment is performed with a super saturated solution without adopting any stirring system. The mechanical forces generated by the stirring have though the disadvantage of damaging the carbon yarns. Indeed, when the rotation of the solution is quite high it can cause the failure of some of the filaments composing the yarn or it can cause an entanglement of the filaments. An additional technical problem faced during the experimental work of the carbon fibers pretreatment was the deposition of the salt on the thermometer inserted in the solution to control the temperature. Although this aspect does not significantly influence the degree of solution concentration as the thermocouple wire has a limited surface, it can affect the accuracy of temperature measurements.

After the  $K_2ZrF_6$  treatment, the fibers were mounted in SEM sample carrier with the aim of observing the effect of the diverse dip-in time on the  $K_2ZrF_6$  crystals distribution. SEM images reported in the results chapter show a remarkable difference between the fibers treated for 1 min compared to the ones treated for 5 mins. First of all, the amount of absorbed salt is, as expected, higher in the 5 min treated C fibers. Not only the quantity but also the quality of the crystals distribution is affected by the treatment duration: in the 1 min treated fibers, the  $K_2ZrF_6$  crystals are mainly located in between the fibers with poor connection with the latter. Instead, after 5 mins treatment, the  $K_2ZrF_6$  crystals are more uniformly distributed with a better connection with the C fibers. Furthermore, their size result to be smaller compared to the C fibers treated for 1 min. Despite the magnetic stirring permit to have a homogeneous solution, the fluid rotation causes mechanical stresses that tend to exfoliate and damage the C fibers. This fact results in a poor quality of the obtainable composite samples as it is showed in the SEM images after the aluminum melting during the DSC tests.



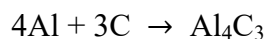
## 5.2 INTERFACE FORMATION

The fiber-matrix interface is the main responsible of the final mechanical proprieties of all types of composites. Although in this work no mechanical tests are carried, it is noteworthy to identify the main interface proprieties that allow a qualitative estimation of the fiber-metal bond strength. The issues associated with the interfaces are the interfacial chemical reaction, lack of wettability with the matrix or degradation of the reinforcement. Wetting of fibers by molten metal is favored by the formation of strong chemical bonds at the interface. The presence of oxide films on the surface of molten metal (Al in this case) and the adsorbed contaminant on the carbon fibers surface generally leads to non-wetting of the fibers with the molten metal. Generally, chemical bonding occurs when the atoms of matrix and reinforcement are in direct contact and is accomplished by exchange of electrons. This type of bonding can be metallic, ionic or covalent. An interface with a metallic bond is more ductile than other bonds, and is desirable in most of the metal matrix composites. However, in this case the direct contact between molten aluminum and carbon fibers can give rise to the formation of  $Al_4C_3$  which can bring to interface embrittlement in case it is present in large amount. Indeed, a large amount of this brittle carbide formed at the interface, can produce destructive notches on the fiber surface. As carbon fiber is a brittle material itself, such notches could increase the rate of destruction of the fiber. High level of aluminum carbide formation may also destroy the integrity of the carbon fiber and cause a loss in tensile strength. Moreover, a heavy reaction rate can make the C/Al interface a strong chemical bond and greatly increase the interfacial shear strength. This will lead to a difficulty for interface debonding, sliding and intensification of stress concentration. However this is not the only aspect to be taken into consideration in this work regarding the interface characteristics: the amount, size and uniformity of  $K_2ZrF_6$  crystals distribution on the carbon fibers play also an important role. Indeed, if the local concentration or the size of those crystals is elevated, it acts as a barrier to chemical bond formation as not all the salt deposited on the fibers will react during the interface formation, thus giving rise to local embrittlement. These aspects will be investigated in the next subsections by discussing the results obtained from the DSC tests and SEM analysis.

### 5.2.1 Interpretation of DSC curves

As already mentioned, the DSC tests completed in this work have both the aim of studying the sequence of reactions that occur between the system of pure aluminum and C fibers treated with  $K_2ZrF_6$  as well as producing small composite samples that will be later observed using optical microscope and SEM. In the thermal curves presented in subsection 4.3.1 of the results chapter, exothermic heat flow is shown down on the y-axis (vice versa the endothermic peaks are shown up in the y-axis). This means that all the larger peaks between  $660^\circ\text{C}$  and  $680^\circ\text{C}$  correspond to the aluminum melting. However, by comparing the different curves it is possible to notice some irregular perturbations in some of those peaks. Indeed, the DSC curve of the pure Al has a perfectly shaped peak while when dealing with aluminum along with treated C fibers, the peaks are always characterized by perturbations in both y-axis directions that indicate both exothermic and endothermic reactions occurring during Al melting and thus interface formation. It is worth noting that even if the process parameters of the fibers treatment and the pure Al amounts are the same, the resulting DSC curve varies in significant way. This makes it difficult to properly evaluate the degree and type of chemical reactions occurring at the interface. One of the main causes of this phenomenon can be related, as already mentioned, to the strong variability of the  $K_2ZrF_6$  crystal deposition on the carbon fibers that is quite difficult to control even if the key parameters are kept steady. The DSC curves also show other very small exothermic peaks before the Al melting zone, probably due to further  $K_2ZrF_6$  decomposition reaction. In fact, according to the phase diagram of the KF-ZrF<sub>4</sub> binary system, the  $K_2ZrF_6$  partly passes in the liquid state (solidus) according to a peritectic reaction at  $587^\circ\text{C}$  and is therefore decomposed into a mixture of a liquid phase L (KF, ZrF<sub>4</sub>) and  $K_3ZrF_7$ . However no reactions at this value of temperature are detected in the performed DSC tests. Focusing on the range of temperatures that goes from  $640^\circ\text{C}$  to  $660^\circ\text{C}$ , it is possible to notice a perturbed region with different exothermic peaks that could be associated with the beginning of the reactions between  $K_2ZrF_6$  and the thin alumina layer on the Al piece. However, due to the imperfect vacuum reached by DSC machine, it could be possible that some small quantity of oxygen might have reacted with the surface

treated carbon fibers. Some of the curves are characterized by two endothermic peaks: one at approximately 668°C and the other at 673°C signifying that both endothermic and exothermic reactions happened in this region. As already mentioned in the state of art chapter, the fact that the free enthalpy of the reaction:



is negative ( $-41 \text{ kcal mol}^{-1}$  at 660°C) suggests that molten aluminum should wet carbon substrates from temperatures beginning at the melting point and this exothermic reaction is probably one of the causes of the double peak presence along with reactions between alumina layer or oxygen and  $\text{K}_2\text{ZrF}_6$ .

After aluminum melting is completed, examining the range between 680°C and 700°C there is in some of the DSC curves a well-defined exothermic peak followed by a perturbed zone. This is most likely the temperature range where reactions between  $\text{K}_2\text{ZrF}_6$  and aluminum come about. Indeed, this salt reacts with molten aluminum to give potassium sodium cryolite according to the following equation:



The resulting potassium aluminum fluoride (potassium cryolite) formed has a melting point of 790°C, therefore this might explain why after reaching the final test temperature of 750°C and starting the cooling of the sample, no evidence of any phase transformation beside the Al solidification, is observed of the DSC curve. Although the ultimate reaction product would be solid and as some time is required for a complete reaction, the potassium cryolite forms a mixture with unreacted  $\text{K}_2\text{ZrF}_6$  that has a lower melting point than aluminum. Hence this could be the presence of the perturbed region after the melting of Al. However no significant variations in the resulting DSC curves occurred in the test conducted at 5°C/min heating rate and with final test temperature of 800°C. One other possible exothermic reaction (as mentioned in the state of art) occurring at the same temperature range, is the formation of the intermetallic compound  $\text{Al}_3\text{Zr}$  at the surface of the carbon fibers:



This suggests that further investigations within this range of temperature should be carried.

### 5.2.2 Microstructure of composite samples

In order to study the microstructure of the different composite samples, Scanning Electron Microscopy (SEM) as well as Energy Dispersive X-ray Spectrometry (EDS) analyses were performed. By observing the images reported in the results chapter it is possible to conduct a qualitative estimation of the main interface characteristics after the DSC tests. From a very first look, it is possible to note the irregular metal infiltration through the carbon fibers filaments as expected. In fact, the use of DSC is not the proper way of obtaining good composite samples. However some interesting features can be derived from these analyses. First of all, by observing the SEM images of the non-polished samples, it is possible to state that although giving a general concept of the infiltration degree, they do not allow to proceed with any further investigation of the fiber-metal interface since the carbon fibers are electric conductors that cause issues when using high level of magnification. However the quality of the obtained images is good enough to note the  $K_2ZrF_6$  crystals deposited on the carbon filaments. In fact they appear to be very bright, irregular and in large quantity. Each crystal of  $K_2ZrF_6$  present on the fiber surface serves as a nucleating center for carbide crystal formation. Large numbers of these carbide crystals or the cohesion bridges strengthen the fiber-matrix bond. Hence, further studies on the distribution of  $K_2ZrF_6$  on the fibers during the dipping process should be taken into account. Also the size of the crystals deposited on the fiber is a factor that can influence the proprieties of the composite. As already mentioned, the improve of the fiber-matrix bonding should be attributed to various causes including fiber surface cleaning, dissolution of aluminum by flourides during fiber molten aluminum contact, decrease of contact angle due to localized heating resulting from exothermic reactions of  $K_2ZrF_6$  with the molten aluminum. However the use of DSC to molten the aluminum is not a good technique that does not lead to an optimum infiltration of the carbon fibers and also the degree of chemical reactions occurring between the salt and the matrix is lower than expected. After mounting and polishing the sample, SEM images show, as expected, several non-homogeneous areas of the sample: there are areas

with fibers concentration while some others appear to be composed by aluminum matrix only. Different flaws such as holes and craters are detected on the sample, probably also due to the polishing phase. Indeed during the grinding process it is likely that not only the matrix, but also the carbon filaments are damaged. This fact is clearly notable in Fig. 4-28 where it is possible to observe a carbon filament consumed in its external substrates in direct contact with the salt. The damage of the carbon filaments may also be caused by chemical reactions occurring at the interface but the SEM images of the non-polished samples do not permit a sufficient level of magnification to observe the carbon filament integrity. In Fig. 4-31 it is possible to observe not only the cross section of the fiber-metal interface but also the points where EDS was conducted. The carbon filament in this case did not present any damage nevertheless displaying a deformation on its radius. The presence of the white salt crystals is evident in the picture. The amount of the salt deposited on the filament resulted to be excessive so it is expected to have a poor quality of the interface. It was conducted an EDS analysis in order to know the nature of the elements at the interface. The resulting spectra reported in Fig. 4-32 suggest as expected to have only carbon presence at the core and pure aluminum far from the interface. However is at the interface that the EDS spectrum shows the most interesting result. In fact it is reported the presence of potassium, zirconium and fluorine as expected due to the  $K_2ZrF_6$  treatment but it is possible to note also the presence of reacted aluminum and the not expected presence of oxygen. As already mentioned the oxygen contamination was taken in consideration due to the non-perfect vacuum of DSC machine, but the amount in which it is detected in this analysis is quite high. This suggests that further investigations of this phenomenon should be carried in order understand if this oxygen layer could be detrimental to the mechanical properties.

It is worth comparing the results obtained from the two different  $K_2ZrF_6$  treatments in order to point out the effects on the final composite samples. As already described in the carbon fibers comparing, there was detected a difference in crystal size and distribution between the fibers treated for 1 min compared to the ones treated for 5 mins. Those differences appear to have an impact also on the features of the final composite samples. By observing the SEM images of the two different composite samples it can be stated that in the samples

where the fibers were treated for 1 min the degree of metal infiltration is lower than the ones where such fibers were treated for 5 minutes. Moreover, in the samples with 1 min treatment also the level of cohesion is lower and it is possible to detect the presence of a higher amount of flaws at the interface.

## 6. CONCLUSIONS AND FUTURE PROSPECTS

In conclusion of this work will be reported the most significant results as well as some future prospects. The first noteworthy conclusion is the one regarding the desizing parameters: it has been shown that optimum results were obtained by treating the carbon fibers at 500 °C for 2 hours in furnace with air circulation. Indeed a higher value of temperature or treatment time would damage the fibers, on the contrary a lower temperature value or lower treatment time has been demonstrated not to be sufficient to completely remove the polymeric coating. As regards the  $K_2ZrF_6$  process parameters, the best results were obtained by treating the carbon fibers with supersaturated solution at 95 °C and a dipping time of 5 minutes. However it is suggested for future treatments the use of a lower solution concentration for the  $K_2ZrF_6$  treatment in order to avoid excessive amount of crystals deposited on the carbon filaments. Indeed it has been revealed that the excessive presence of the salt at the fiber-metal interface resulted to cause a local embrittlement. Moreover, it is suggested to improve the temperature control system of the solution. This in fact is the main parameter in controlling the homogeneity and the size of the crystals distribution on the carbon filaments surface. A better treatment could be obtained with a continuous system so it proposed for future works a study of its feasibility.

## 7. REFERENCES

- [1] A. Mertens, H.-M. Montrieux, J. Halleux, J. Lecomte-Beckers, F. Delannay, Processing of Carbon Fibers Reinforced Mg Matrix Composites Via Pre-infiltration with Al, *Journal of Materials Engineering and Performance*. 21 (2012) 701–706. doi:10.1007/s11665-012-0177-4.
- [2] C.T. Lynch, *Metal Matrix Composites*, (n.d.) 181.
- [3] M.U. Islam and W. Wallace, Carbon Fibre Reinforced Aluminium Matrix Composites. A Critical Review, *Adv. Mater. Manuf. Process.*, Vol 3 (No. 1), 1988, p 1, n.d.
- [4] M.F. Amateau, Progress in the Development of Graphite-Aluminum Composites Using Liquid Infiltration Technology, *J. Compos. Mater.*, Vol 10, Oct 1976, p 279, n.d.
- [5] M. Yoshida, S. Ikegami, T. Ohsaki, and T. Ohkita, Studies on Ion-Plating Process for Making Carbon Fiber Reinforced Aluminum and Properties of the Composites, in *Proceedings of the 24th National SAMPE Symposium*, Vol 24, Society for the Advancement of Material and Process Engineering, 1979, p 1417, (n.d.).
- [6] R.J. Sample, R.B. Bhagat, and M.F. Amateau, High Pressure Squeeze Casting of Unidirectional Graphite Fiber Reinforced Aluminum Matrix Composites, in *Cast Reinforced Metal Composites*, S.G. Fishman and A.K. Dhingra, Ed., ASM INTERNATIONAL, 1988, p 179, (n.d.).
- [7] R.B. Francini, Characterization of Thin-Wall Graphite/Metal Pultruded Tubing, in *Testing Technology of Metal Matrix Composites*, STP 964, P.R. Di- Giovanni and N.R. Adsit, Ed., American Society for Testing and Materials, 1988, p 396, (n.d.).
- [8] L.M. Sheppard, Challenges Facing the Carbon Industry, *Ceram. Bull.*, Vol 67 (No. 12), 1988, p 1897, (n.d.).
- [9] B.J. Maclean and M.S. Misra, Thermal- Mechanical Behavior of Graphite/ Magnesium Composites, in *Mechanical Behavior of Metal-Matrix Composites*, J.E. Hack and M.F. Amateau, Ed., The Metallurgical Society of AIME, 1982, p 195, (n.d.).
- [10] H.A. Katzman, Fibre Coatings for the Fabrication of Graphite-Reinforced Magnesium Composites, *J. Mater. Sci.*, Vol 22, 1987, p 144, n.d.
- [11] J.C. Viala, P. Fortier, G. Claveyrolas, H. Vincent, J. Bouix, Effect of magnesium on the composition, microstructure and mechanical properties of carbon fibres, *Journal of Materials Science*. 26 (1991) 4977–4984. doi:10.1007/BF00549880.
- [12] J.C. VIALA, G. CLAVEYROLAS, F. BOSSELET, J. BOUIX, The chemical behaviour of carbon fibres in magnesium base Mg-Al alloys, (n.d.) 13.
- [13] Feldhoff, Pippel, Woltersdorf, Carbon-fibre reinforced magnesium alloys: nanostructure and chemistry of interlayers and their effect on mechanical properties, *Journal of Microscopy*. 196 (1999) 185–193. doi:10.1046/j.1365-2818.1999.00618.x.
- [14] J.P. Rocher, J.M. Quenisset, R. Naslain, Wetting improvement of carbon or silicon carbide by aluminium alloys based on a K 2 ZrF 6 surface treatment: application to composite material casting, *Journal of Materials Science*. 24 (1989) 2697–2703.
- [15] S. Schamm, R. Fedou, J.P. Rocher, J.M. Quenisset, R. Naslain, The K 2 ZrF 6 wetting process: Effect of surface chemistry on the ability of a SiC-Fiber preform to be impregnated by aluminum, *Metallurgical Transactions A*. 22 (1991) 2133–2139.



- [16] X. Chen, G. Zhen, Z. Shen, A TEM study of the interfaces and matrices of SiC-coated carbon fibre/aluminium composites made by the K<sub>2</sub>ZrF<sub>6</sub> process, *Journal of Materials Science*. 31 (1996) 4297–4302.
- [17] S. Schamm, Y.L. Petitcorps, R. Naslain, Compatibility Between SiC Filaments and Aluminium in the K<sub>2</sub>ZrF<sub>6</sub> Wetting Process and its Effect on Filament Strength, (n.d.) 19.
- [18] S. Schamm, J.P. Rocher, R. Naslain, Physicochemical Aspects of the K<sub>2</sub>ZrF<sub>6</sub> Process Allowing the Spontaneous Infiltration of SiC (or C) Preforms by Liquid Aluminium, in: A.R. Bunsell, P. Lamicq, A. Massiah (Eds.), *Developments in the Science and Technology of Composite Materials*, Springer Netherlands, Dordrecht, 1989: pp. 157–163. doi:10.1007/978-94-009-1123-9\_21.
- [19] P. MORGAN, CARBON FIBERS and their COMPOSITES, (2005) 1147.
- [20] X. Huang, Fabrication and Properties of Carbon Fibers, *Materials*. 2 (2009) 2369–2403. doi:10.3390/ma2042369.
- [21] Chang TC, Plasma surface treatment in composites manufacturing, *J Ind Technol*, 15(1), 7, Nov 1998–Jan 1999, (n.d.).
- [22] R.E. Allred, S.P. Wesson, Surface Characterization of Sized and Desized Toray M40J Carbon Fibers, (n.d.) 11.
- [23] C. Salmon, Elaboration et caractérisation de composites Pb/carbone et Pb/verre en vue de leur utilisation comme anode d'électrolyse, Master Thesis, Université catholique de Louvain, Louvain-la-Neuve, 1995, n.d.
- [24] Z. Dai, F. Shi, B. Zhang, M. Li, Z. Zhang, Effect of sizing on carbon fiber surface properties and fibers/epoxy interfacial adhesion, *Applied Surface Science*. 257 (2011) 6980–6985. doi:10.1016/j.apsusc.2011.03.047.
- [25] S.N. Patankar, V. Gopinathan, P. Ramakrishnan, Processing of carbon fibre reinforced aluminium composite using K<sub>2</sub>ZrF<sub>6</sub> treated carbon fibres: a degradation study, *Journal of Materials Science Letters*. 9 (1990) 912–913.
- [26] H.A. Katzman, Fibre coatings for the fabrication of graphite-reinforced magnesium composites, *Journal of Materials Science*. 22 (1987) 144–148. doi:10.1007/BF01160563.
- [27] S. Wang, Z.-H. Chen, W.-J. Ma, Q.-S. Ma, Influence of heat treatment on physical–chemical properties of PAN-based carbon fiber, *Ceramics International*. 32 (2006) 291–295. doi:10.1016/j.ceramint.2005.02.014.
- [28] J.P. Rocher, J.M. Quenisset, R. Naslain, A new casting process for carbon (or SiC-based) fibre-aluminium matrix low-cost composite materials, *Journal of Materials Science Letters*. 4 (1985) 1527–1529.
- [29] Studies on carbon fibre reinforced aluminium composite processed using pre-treated carbon fibres, (n.d.) 7.
- [30] E. DE LAMOTTE, K. PHILLIPS, A. J. PERRY and H. R. KILLIAS, *J. Mater. Sci. Lett.* 7 (1972) 346., (n.d.).
- [31] A. P. LEVITT and H. E. BAND, US Pat. no. 4 157409, 5 June 1979., (n.d.).
- [32] E. G. KENDALL and R. T. PEPPER, US Pat. no. 4082864, 4 April 1978, (n.d.).
- [33] H. LUNDIN, U.S. Pat. 2686354, October 1949., (n.d.).
- [34] N. A. BUSHE and M. E. SEMENOV, *Lileinoe Proizv* 2 (1962) 15., (n.d.).

- [35] J. Hála, S.A. Johnson, eds., Halides, oxyhalides and salts of halogen complexes of titanium, zirconium, hafnium, vanadium, niobium and tantalum, Pergamon Press, Oxford, 1989.
- [36] C. Körner, W. Schäff, M. Ottmüller, R.F. Singer, Carbon Long Fiber Reinforced Magnesium Alloys, *Advanced Engineering Materials*. 2 (2000) 327–337. doi:10.1002/1527-2648(200006)2:6<327::AID-ADEM327>3.0.CO;2-W.